UNIVERSIDADE FEDERAL RURAL DO SEMI-ÁRIDO
PRÓ-REITORIA DE PESQUISA E PÓS-GRADUAÇÃO
PROGRAMA DE PÓS-GRADUAÇÃO EM FITOTECNIA
DOUTORADO EM FITOTECNIA

BRUNO CAIO CHAVES FERNANDES

CHARACTERIZATION OF EUCALYPTUS WOOD-DERIVED BIOCHAR AND ITS EFFECTS ON HEXAZINONE BEHAVIOR IN SOIL

MOSSORÓ/RN
2019

BRUNO CAIO CHAVES FERNANDES

CHARACTERIZATION OF EUCALYPTUS WOOD-DERIVED BIOCHAR AND ITS EFFECTS ON HEXAZINONE BEHAVIOR IN SOIL

Thesis submitted to the Federal Rural University of the Semi-Arid, in partial fulfillment of the requirements for the degree of Doctor in Plant Science

Research area: Weed management

Advisor: Daniel Valadão Silva, Prof. Dr

Co-advisors: Kassio Ferreira Mendes, Prof. Dr
Matheus de Freitas Souza, Dr

MOSSORÓ/RN
2019

Dados Internacionais de Catalogação na Publicação (CIP)
Biblioteca Central Orlando Teixeira (BCOT)

F363c Fernandes, Bruno Caio Chaves Fernandes .
Characterization of eucalyptus wood-derived biochar and its effects on hexazinone behavior in soil / Bruno Caio Chaves Fernandes Fernandes. - 2019 .
68 f. : il.

Orientador: Daniel Valadão Silva Silva .
Coorientador: Kassio Ferreira Mendes Mendes .
Tese (Doutorado) - Universidade Federal Rural do Semi-árido, Programa de Pós-graduação em Fitotecnia, 2019 .

1. Herbicida. 2. lixiviação. 3. persistência. 4. poluente orgânico . 5. sorvente. I. Silva , Daniel Valadão Silva, orient. II. Mendes , Kassio Ferreira Mendes, co-orient. III. Título.

O serviço de Geração Automática de Ficha Catalográfica para Trabalhos de Conclusão de Curso (TCC´s) foi desenvolvido pelo Instituto de Ciências Matemáticas e de Computação da Universidade de São Paulo (USP) e gentilmente cedido para o Sistema de Bibliotecas da Universidade Federal Rural do Semi-Árido (SISBI-UFERSA), sendo customizado pela Superintendência de Tecnologia da Informação e Comunicação (SUTIC) sob orientação dos bibliotecários da instituição para ser adaptado às necessidades dos alunos dos Cursos de Graduação e Programas de Pós-Graduação da Universidade.

BRUNO CAIO CHAVES FERNANDES

CHARACTERIZATION OF EUCALYPTUS WOOD-DERIVED BIOCHAR AND ITS EFFECTS ON HEXAZINONE BEHAVIOR IN SOIL

Thesis submitted to the Federal Rural University of the Semi-Arid, in partial fulfillment of the requirements for the degree of Doctor in Plant Science.

Line of research: Weed management

APPROVED IN: 19 / 12 / 2019.

DEFENSE COMMITTEE MEMBERS

Daniel Valadão Silva, Prof. Dr (UFERSA)
Advisor

Kassio Ferreira Mendes, Prof. Dr (UFV)
External committee member

Eulene Francisco da Silva, Profª. Dra (UFERSA)
External committee member

Evander Alves Ferreira, Prof. Dr. (UFMG)
External committee member

Ana Beatriz Rocha de Jesus Passos, Dra (UFERSA)
External committee member

To my beloved parents, João Batista Chaves and Dina Geruza Fernandes Chaves, for all their dedication, education and love. To you I dedicate all my victories.

DEDICATION

ACKNOWLEDGEMENTS

To God, for giving me strength, health, and knowledge.;

Universidade Federal Rural do Semi-Árido and to the Department of Agronomic and Forest Sciences, for the release and incentive to do the doctorate;

PPGF/UFERSA Postgraduate Program in Phytotechnics - Mossoró-RN, for the opportunity to perform doctorate, even though I am not an agronomist;

My parents, João and Dina Geruza, for their education, love, dedication and for always believing in me, my biggest supporters;

My uncles Raimundo Abrantes and Arimar Chaves and my cousins Marcia, Joana, and Márly, with the usual affection, support during my education and immense patience;

To my teacher and advisor, Daniel Valadão Silva, for the trust and opportunity.

To my teacher and co-advisor Kassio Mendes and all the staff of CENA for having welcomed me, helped in my academic growth and the great friendship that remained. Thank you for all your patience and dedication. Thanks also in particular to Professor Valdemar Tornisielo and Vanessa Takeshita;

To my friends Taliane Teófilo, Tatiane Severo, and Matheus Freitas for their companionship, strength, patience, and help. Be sure that you were essential to this work. My eternal thanks;

Thank the members of the examination board teachers;

My girlfriend, Barbara Fonseca, thank you for the companionship and patience throughout this journey;

To work friends Christiane, Juliana, Renan, Priscila, Lidiane and especially to the great friend Paulo

There is no such thing as a process of neutral education, education, or it functions as an instrument that is used to facilitate integration of generations into logic of the present system and bring conformity with it, or it becomes the “practice of freedom”, form whereby men and women critically deal with reality and discover how to participate in transforming their world.

Paulo Freire

ABSTRACT

FERNANDES, Bruno Caio Chaves. **Characterization of eucalyptus wood-derived biochar and its effects on hexazinone behavior in soil.** 2019. 68p. Thesis (D.Sc. in Plant Science) – Federal Rural University of the Semi-Arid (UFERSA), Mossoró-RN, 2019.

Biochar is a product rich in carbon produced from pyrolysis of organic materials in an environment with limited oxygen or anoxic conditions. The pyrolysis temperature of material has a direct influence on the properties of biochar and, consequently, on its potential for agricultural and environmental use. In this research, the biochar characteristics of eucalyptus wood residues produced at different pyrolysis temperatures and their relationship with the behavior of herbicide hexazinone in soil were evaluated. Initially, biochars were produced at temperatures of 450, 550, 650, 750, 850 and 950 °C on the hydrogen potential (pH value), electrical conductivity (EC), ash content, yield, volatile matter (VM) content, elemental analysis, Fourier transform-infrared spectroscopy (FT-IR), X-ray diffraction, scanning electron microscopy (SEM), specific surface area (SSA) and micropore volume (MV) (by N_2 adsorption) of eucalyptus wood-derived biochar. In the second stage, sorption/desorption experiments were executed using the batch equilibrium method, leaching in glass columns and distribution in biometric flasks with biochars produced between temperatures of 650 to 950 °C. The results showed a positive correlation of pyrolysis temperature with pH value, EC and elemental carbon, and a negative correlation with yield, MV, oxygen, elemental hydrogen, SSA, H/C, O/C and (O+N)/C ratios. The Principal component analysis showed that the highest polarity index (O+N/C), ash content, and N/C ratio associated with a low H/C ratio were the characteristics that had the greatest influence on increasing sorption, promoting a reduction in leaching and availability of hexazinone. The biochars produced at 850 and 950 °C obtained the highest sorption, reducing leaching by more than 80% and hexazinone availability by more than 46%. The addition of biochar was efficient in decreasing the mobility and availability of hexazinone in the soil, reducing the risk of environmental contamination of this herbicide. However, the lowest available amount of hexazinone in the soil can reduce the effectiveness of weed control in field conditions

Keywords: Herbicide, leaching, organic pollutant, persistence and sorbent

RESUMO

FERNANDES, Bruno Caio Chaves. **Caracterização do *biochar* derivado de madeira de eucalipto e seus efeitos sobre o comportamento do hexazinone no solo.** 2019. 68f. Tese (Doutorado em Fitotecnia) – Universidade Federal Rural do Semi-Árido (UFERSA), Mossoró-RN, 2019.

O *biochar* é um produto rico em carbono produzido a partir pirólise de materiais orgânicos em um ambiente com condições limitadas de oxigênio ou anóxicas. A temperatura de pirólise do material tem influência direta nas propriedades do biochar e, consequentemente, no seu potencial de seu uso agrícola e ambiental. Nesta pesquisa foram avaliadas as características de *biochar* de resíduos de madeira de eucalipto produzido em diferentes temperaturas de pirólise e sua relação com o comportamento do herbicida hexazinone no solo. Inicialmente realizou-se produção dos *biochars* nas temperaturas de 450, 550, 650, 750, 850 e 950°C e foram determinados o pH, CE, teor de cinzas, rendimento, materiais voláteis (TMV), análise elementar (CHN-O), espectroscopia no infravermelho por transformada de Fourier, área de superfície específica e volume de microporos, difração de raio-X e microscopia eletrônica de varredura. Na segunda etapa foram realizados experimentos de sorção/dessorção foram obtidos pelo método de equilíbrio em lotes, de lixiviação em colunas de vidros e o de distribuição em frascos biométricos com os *biochars* produzido entre as temperaturas de 650 a 950°C. Os resultados mostraram uma correlação positiva da temperatura de pirólise com o pH, CE e com o carbono elementar, mantendo uma correlação negativa com o rendimento, TMV, oxigênio, hidrogênio elementar, na relação H/C, O/C e (O+N)/C e na área de superfície especifica. A análise de componentes principais mostrou que o maior índice de polaridade (O+N/C), teor de cinzas e relação N/C associado com uma baixa relação de H/C foram as características que tiveram maior influência no aumento da sorção, promovendo uma redução na lixiviação e na disponibilidade do hexazinone. Os *biochars* produzidos à 850 e 950 °C foram os que obtiveram maior sorção, reduzindo em mais de 80% a lixiviação e em mais de 46% a disponibilidade do hexazinone. A adição do *biochar* foi eficiente para diminuiu a mobilidade e disponibilidade do hexazinone no solo, reduzindo o risco de contaminação ambiental desse herbicida. No entanto, a menor quantidade disponível de hexazinone no solo pode reduzir a eficácia no controle de plantas daninhas em condição de campo.

Palavras-chave: Herbicida, lixiviação, persistência, poluente orgânico e sorvente.

LIST OF FIGURES

CHAPTER I

CHAPTER II

LIST OF TABLES

CHAPTER I

CHAPTER II

SUMMARY

INTRODUCTION

The extensive and sometimes inappropriate use of herbicides in recent decades has led to contamination of soils, surface, and groundwater, becoming one of the main environmental issues in the world. Herbicides even at low concentrations (ng L^{-1} ou μg L^{-1}) are capable of causing harmful effects to the aquatic ecosystem and human health (MEFFE; BUSTAMANTE, 2014; LEI et al., 2015), raising concerns about the risks and effects of their contamination.

Among herbicides, hexazinone has high water solubility (33.000 mg L^{-1} a 25°C), (KIM et al., 2018), low sorption (Kf = 0,2 mg^{1-n} L^n kg^{-1}) in the soils (PEREIRA-JUNIOR et al., 2015) and moderate persistence (105 days) (PPDB, 2019). These characteristics favor the vertical (leaching) and horizontal (surface runoff) movement of hexazinone in soil, increasing risk of contamination of water resources (CLOSE; SKINNER, 2012; MACHADO et al., 2016). Hexazinone [3-cyclohexyl-6-(dimethylamino)-1-methyl-1,3,5-triazine-2-4(1*H*,3*H*) dione] is a broad-spectrum herbicide belonging to the group of triazinones used worldwide for the control of weeds in agriculture, railways and highways (MEI et al., 2012; PPDB, 2019).

Currently, several methods are being used to reduce contamination of soils and water resources, such as precipitation (MEUNIER et al., 2006), ion exchange (DESAI et al., 2016) membrane filtration (KOYUNCU et al., 2008), coagulation (FERNIZA-GARCÍA et al., 2017), phytoremediation (PAZ-FERREIRO et al., 2014) and adsorption (YU et al., 2016). The use of biochar, as a adsorbent, has attracted the attention of several researchers for the removal of herbicides due to its high efficiency, low cost and environmental compatibility (DAI et al., 2019).

The biochar is a carbon rich byproduct produced from the pyrolysis of organic waste (for example, crop residues, wood wastes and animal) in absence of oxygen (TAN et al., 2015; KHORRAM et al., 2016; XIAO et al., 2017). Use of biochar in soils shows many advantages, including improved soil structure and the potential to reduce leaching of organic pollutants (GÁMIZ et al., 2019). This is due to its properties, such as a relatively high surface area, high pH, high content of organic C and the presence of functional groups that can bind to contaminants (MAYAKADUWA et al., 2016). Normally, biochar increases the sorption of herbicides in soil and, consequently, reduces its leaching and slows its degradation (LIU et al., 2018).

Temperature of pyrolysis and the raw material are considered the main factors that affect physicochemical properties of the biochar (GAI et al., 2014), that affect the herbicide sorption capacity (WANG et al., 2013, TRIGO et al., 2016; WEI et al., 2017). Temperature is

one of the main factors in properties of biochar, such as specific surface area (SSA), microporosity and stability. With the increase in pyrolysis temperature, increase in aromaticity and SSA were observed (WANG et al., 2010; ZHAO et al., 2018). The characteristics of raw material's biomass confer specific properties of the biochar, such as ash content and its elemental constituents and density (TRIGO et al., 2016). All of these biochar characteristics can affect the sorption of herbicides in soil, which determines their mobility and ability to mitigate the contamination of surface and groundwater.

The strong sorption of herbicides can be problematic when the biochar is used as a soil modifier, it can reduce the effectiveness of herbicides applied in pre-emergence, requiring the farmer to use higher doses to obtain the same effect (GRABER et al., 2012). However, strong sorption also means that the biochar can function as an efficient filter material, which can be used to reduce herbicide leaching in diffuse and point sources, such as in agricultural ditches and drainage systems and in areas where herbicides are manipulated and potentially spilled (CEDERLUND et al., 2017).

Increased interest in the application of biochar to remove organic pollutants, especially soluble herbicides such as hexazinone, is essential to determine the ideal pyrolysis conditions to produce the biochar with the most suitable properties to reduce the risk of environmental contamination associated with the use of herbicides. Suliman et al. (2016) reported better sorbent properties of biochar produced at higher temperatures, as a consequence of greater surface area and microporosity. However, Yavari et al. (2016) showed that lower conversion temperature (300 ° C) increases the functional groups on the surface of biochars, increasing the sorption efficiency of polar herbicides, imazapic, and imazapyr. Yang et al. (2010) considered that temperature is more important than raw material in the effectiveness of biochar in the treatment of soil contaminated with pesticides.

The characterization of physicochemical properties of biochars produced from any raw material, in particular under a certain set of pyrolysis conditions, allows the understanding of its most relevant properties and the most suitable purpose for its use (SULIMAN et al., 2016). Wood harvest residues from planted forests are one of the most abundant sources of biomass available for biochar production, but little is known about the influence of pyrolysis temperature on their properties and how this influences the behavior of herbicides in soils.

The mobile and persistent nature of hexazinone in the environment makes it necessary to explore strategies to reduce its leaching in soils. Specifically, few pieces of information are available on the role of eucalyptus wood biochar in the sorption, distribution and mobility of hexazinone in the environment. Therefore, this study investigated the physicochemical

properties of eucalyptus wood-derived biochar produced at different pyrolysis temperatures to determine the effects of its properties on the sorption/desorption, leaching, and distribution of hexazinone.

.

REFERENCE

CEDERLUND, H. et al. Effects of a wood-based biochar on the leaching of pesticides chlorpyrifos, diuron, glyphosate and MCPA. **Journal of Environmental Management**, v. 191, p. 28-34, 2017.

CLOSE, M. E.; SKINNER, A. Sixth national survey of pesticides in groundwater in New Zealand. **New Zealand Journal of Marine and Freshwater Research**, v. 46, n. 4, p. 443-457, 2012.

DAI, Y et al. The adsorption, regeneration and engineering applications of biochar for removal organic pollutants: A review. **Chemosphere**, v. 223, p. 12-27, 2019.

DESAI, A. V. et al. A water-stable cationic metal–organic framework as a dual adsorbent of oxoanion pollutants. **Angewandte Chemie International Edition**, v. 55, n. 27, p. 7811-7815, 2016.

FERNIZA-GARCÍA, F. et al. Removal of Pb, Cu, Cd, and Zn present in aqueous solution using coupled electrocoagulation-phytoremediation treatment. **International Journal of Electrochemistry**, v. 2017, p. 1-11, 2017.

GAI, X. et al. Effects of feedstock and pyrolysis temperature on biochar adsorption of ammonium and nitrate. **PloS One**, v. 9, n. 12, p. 1-19, 2014.

GÁMIZ, B. et al. Changes in sorption and bioavailability of herbicides in soil amended with fresh and aged biochar. **Geoderma**, v. 337, p. 341-349, 2019.

GRABER, E. R. et al. High surface area biochar negatively impacts herbicide efficacy. **Plant and Soil**, v. 353, n. 1-2, p. 95-106, 2012.

JONES, D. L. et al. Biochar mediated alterations in herbicide breakdown and leaching in soil. **Soil biology and Biochemistry**, v. 43, n. 4, p. 804-813, 2011.

KEIZER, J. P. et al. Long-term ground water quality impacts from the use of hexazinone for the commercial production of lowbush blueberries. **Groundwater Monitoring & Remediation**, v. 21, n. 3, p. 128-135, 2001.

KHORRAM, M. et al. Biochar: a review of its impact on pesticide behavior in soil environments and its potential applications. **Journal of Environmental Sciences**, v. 44, p. 269-279, 2016.

KOELMANS, A. A. et al. Black carbon: the reverse of its dark side. **Chemosphere**, v. 63, n. 3, p. 365-377, 2006.

KOYUNCU, I. et al. Removal of hormones and antibiotics by nanofiltration membranes. **Journal of Membrane Science**, v. 309, n. 1-2, p. 94-101, 2008.

LEHMANN, J.; JOSEPH, S. (Ed.). **Biochar for Environmental management: science, technology and implementation**. New York: Routledge, 2015, 943p.

LEI, M. et al. Overview of emerging contaminants and associated human health effects. **BioMed Research International**, v. 2015, p. 1-12, 2015.

LIU, Y. et al. Impact of biochar amendment in agricultural soils on the sorption, desorption, and degradation of pesticides: a review. **Science of the Total Environment**, v. 645, p. 60-70, 2018.

LOHMANN, R. The emergence of black carbon as a super-sorbent in environmental chemistry: The end of octanol? **Environmental Forensics**, v. 4, n. 3, p. 161-165, 2003.

MACHADO, C. S. et al. Chemical contamination of water and sediments in the Pardo River, São Paulo, Brazil. **Procedia Engineering**, v. 162, p. 230-237, 2016.

MAYAKADUWA, S. S. et al. Equilibrium and kinetic mechanisms of woody biochar on aqueous glyphosate removal. **Chemosphere**, v. 144, p. 2516-2521, 2016.

MEFFE, R.; BUSTAMANTE, I. Emerging organic contaminants in surface water and groundwater: a first overview of the situation in Italy. **Science of the Total Environment**, v. 481, p. 280-295, 2014.

MEUNIER, N. et al. Comparison between electrocoagulation and chemical precipitation for metals removal from acidic soil leachate. **Journal of Hazardous Materials**, v. 137, n. 1, p. 581-590, 2006.

PAZ-FERREIRO, J. et al. Use of phytoremediation and biochar to remediate heavy metal polluted soils: a review. **Solid Earth**, v. 5, n. 1, p. 65-75, 2014.

PEREIRA-JUNIOR, E. V. et al. Effects of soil attributes and straw accumulation on the sorption of hexazinone and tebuthiuron in tropical soils cultivated with sugarcane. **Journal of Environmental Science and Health, Part B**, v. 50, n. 4, p. 238-246, 2015.

ROUSIS, N. I. et al. Monitoring a large number of pesticides and transformation products in water samples from Spain and Italy. **Environmental Research**, v. 156, p. 31-38, 2017.

RUBIO-BELLIDO, M. et al. Assessment of soil diuron bioavailability to plants and microorganisms through non-exhaustive chemical extractions of the herbicide. **Geoderma**, v. 312, p. 130-138, 2018.

SHANER, D. L. et al. **Herbicide handbook**. Weed Science Society of America, 2014.

SOPEÑA, F. et al. Assessing the chemical and biological accessibility of the herbicide isoproturon in soil amended with biochar. **Chemosphere**, v. 88, n. 1, p. 77-83, 2012.

SULIMAN, W. et al. Influence of feedstock source and pyrolysis temperature on biochar bulk and surface properties. **Biomass and Bioenergy**, v. 84, p. 37-48, 2016.

SUN, J. et al. Biochars derived from various crop straws: characterization and Cd (II) removal potential. **Ecotoxicology and Environmental Safety**, v. 106, p. 226-231, 2014.

TAN, X. et al. Biochar-based nano-composites for the decontamination of wastewater: a review. **Bioresource Technology**, v. 212, p. 318-333, 2016.

TRIGO, C. et al. Influence of pyrolysis temperature and hardwood species on resulting biochar properties and their effect on azimsulfuron sorption as compared to other sorbents. **Science of the Total Environment**, v. 566, p. 1454-1464, 2016.

WANG, H. et al. Sorption of the herbicide terbuthylazine in two New Zealand forest soils amended with biosolids and biochars. **Journal of Soils and Sediments**, v. 10, n. 2, p. 283-289, 2010.

WANG, Y. et al. Comparisons of biochar properties from wood material and crop residues at different temperatures and residence times. **Energy & Fuels**, v. 27, n. 10, p. 5890-5899, 2013.

WEI, L. et al. Biochar characteristics produced from rice husks and their sorption properties for the acetanilide herbicide metolachlor. **Environmental Science and Pollution Research**, v. 24, n. 5, p. 4552-4561, 2017.

XIAO, R. et al. Recent developments in biochar utilization as an additive in organic solid waste composting: A review. **Bioresource Technology**, v. 246, p. 203-213, 2017.

YANG, X. B. et al. Influence of biochars on plant uptake and dissipation of two pesticides in an agricultural soil. **Journal of Agricultural and Food Chemistry**, v. 58, n. 13, p. 7915-7921, 2010.

YAVARI, S. et al. Sorption-desorption mechanisms of imazapic and imazapyr herbicides on biochars produced from agricultural wastes. **Journal of Environmental Chemical Engineering**, v. 4, n. 4, p. 3981-3989, 2016.

YU, J. et al. Removal of mercury by adsorption: a review. **Environmental Science and Pollution Research**, v. 23, n. 6, p. 5056-5076, 2016.

ZAMA, E. F. et al. The role of biochar properties in influencing the sorption and desorption of Pb (II), Cd (II) and As (III) in aqueous solution. **Journal of Cleaner Production**, v. 148, p. 127-136, 2017.

ZHAO, B. et al. Effect of pyrolysis temperature, heating rate, and residence time on rapeseed stem derived biochar. **Journal of Cleaner Production**, v. 174, p. 977-987, 2018.

CHAPTER I-IMPACT OF PYROLYSIS TEMPERATURE ON THE PROPERTIES OF EUCALYPTUS WOOD-DERIVED BIOCHAR

ABSTRACT

Pyrolysis conditions directly influence biochar properties and, consequently, influence the potential use of biochars. In this study, we evaluated the effects of different pyrolysis temperatures (450, 550, 650, 750, 850 and 950 °C) on the hydrogen potential (pH value), electrical conductivity (EC), ash content, yield, volatile matter (VM) content, elemental analysis, Fourier transform-infrared spectroscopy (FT-IR) results, X-ray diffraction results, scanning electron microscopy (SEM) results, specific surface area (SSA) and micropore volume (MV) (by N^2 adsorption) of eucalyptus wood-derived biochar. The degree of linear association between pyrolysis temperatures and biochar properties was examined using the Pearson correlation coefficient. The results showed a positive correlation of the pyrolysis temperature with pH value, EC and elemental carbon but showed a negative correlation with yield, VM content, elemental oxygen, elemental hydrogen, SSA and the H/C, O/C and (O+N)/C ratios. The FT-IR data indicate an increase in aromaticity and a decrease in polarity of high-temperature biochar. The increased pyrolysis temperature causes the loss of cellulose and crystalline mineral components, as indicated by X-ray diffraction analysis and SEM images. These results indicate that changing the pyrolysis temperature enables the production of a biochar from the same raw material with a wide range of physicochemical properties, which allows its use in various types of agricultural and environmental activities.

Keywords: Adsorbent materials, Characterization, Charcoal, Chemical composition, Eucalyptus waste and Surface functional group.

1 INTRODUCTION

Biochar is a carbon-rich porous material produced by the pyrolysis of organic materials under an environment with limited oxygen or anoxic conditions (RONSSE et al., 2013; LIN et al., 2017). Its use is a potential alternative that can promote benefits in agricultural yield, carbon sequestration, waste management, clean energy production and reclamation of degraded areas (KOOKANA et al., 2011; ZHAO et al., 2018; MANNA; SINGH, 2019).

A wide variety of biomass feedstocks can be used to produce biochar. Large amounts of agricultural waste are generated worldwide and are not always properly discarded or recycled. Wood production in Brazil annually generates approximately 50.8 million m^3 of lignocellulosic waste (IPEA, 2012); eucalyptus is the most cultivated forest species with 7.83 million hectares of planted trees (IBÁ, 2017) and contributes largely to the creation of this lignocellulosic waste. Waste conversion into biochar can reduce the volume of lignocellulosic waste and can contribute to power generation, improvements in crop nutrient efficiency, elimination of pathogens and generation of products with high agronomic and environmental value (SPOKAS et al., 2012).

The properties and functions of biochars are highly dependent on the raw materials and production conditions. The pyrolysis temperature affects the biochar characteristics and texture (TRIPATHI et al., 2016). Several studies have evaluated the relationships between various biochars and their pyrolysis conditions (AL-WABEL et al., 2013; LIU et al., 2014; SULIMAN et al., 2016; YANG et al., 2019). Huff et al. (2014) reported the increase in aromaticity of biochars from pine wood, peanut shell and bamboo biomass at higher temperatures, and they reported on the possibility of using these biochars for the potential removal of organic molecules. Jones et al. (2011) studied the effect of biochar from eucalyptus wood (*Eucalyptus marginatus*) on simazine leaching and degradation, and they noted that the high sorption of this product reduced its mobility; however, herbicide persistence was increased with the reduced availability for microorganisms in soil.

The use of biochar produced from eucalyptus waste, which is an abundant material that is easy to acquire in Brazil, can improve the disposal of waste from the forest industry. However, it is necessary to determine the best conditions for obtaining the material. Therefore, this research evaluated the effects of different pyrolysis temperatures on the properties of eucalyptus-derived biochar as a method to optimize its use in agronomic and environmental applications.

2 MATERIAL AND METHODS

2.1 Biochar production

Eucalyptus residue was acquired from a clone wood that was the result of crossing *Eucalyptus urophylla* x *Eucalyptus grandi*. The material was crushed into small pieces using a TECNAL knife mill (Willey TE 340, Piracicaba, Brazil). Then, the biomass powder was passed through a 2-mm sieve and dried in an oven with air circulation at 103 ± 2 °C. Biomass pyrolysis was performed in a metal cylinder inside a muffle furnace (Q318M, Quimis, Diadema, São Paulo, Brazil). Carbonization was performed at final temperatures of 450, 550, 650, 750, 850 and 950 °C. The amount of residue used for each repetition was 200 ± 10 g; the temperature was increased by 1.7 °C min^{-1} and maintained at the final temperature for 1 h under a limited supply of air. After cooling, the biochar samples were ground, sieved (20-mesh, <0.9 mm) and stored in a desiccator. The charcoal yield was calculated by its mass difference in relation to the dry wood.

2.2 Biochar characterization

2.2.1 Elemental and energy dispersion X-ray fluorescence spectrometry analyses

An elemental analyzer was used to determine the amount of carbon (C), oxygen (O), hydrogen (H) and nitrogen (N) (Vario MACRO Cube, Elementar, Cheadle Hulme, United Kingdom). One hundred milligrams of each dried biochar sample were weighed in the tin capsule; next, the capsule was closed and placed in the apparatus, which operates by subjecting the samples to combustion under a pure oxygen atmosphere (99,999%). Gases formed by this combustion were measured with a thermal conductivity detector. The O content was estimated by mass balance: O =100-(C+H+N+mineral).

The inorganic mineral content was determined by energy dispersive X-ray fluorescence spectrometry (EDXRF). One gram of biochar sample was weighed and ground; next, the biochar sample was packed in a 20 mm diameter polyethylene beaker and covered with a 6-µm thick polypropylene film. Samples were irradiated in triplicate for 300 s under vacuum using an EDXRF instrument (EDXRF-720, Shimadzu, Kyoto, Japan). Samples were irradiated using an X-ray tube operated at 15 kV (Na a Sc) and 50 kV (Ti a U). The current was adjusted automatically (1 mA maximum). A 10 mm collimator was used. Detection was performed with a liquid nitrogen-cooled Si (Li) detector.

2.2.2 Ash and volatile matter (VM) contents

Ash and VM contents were evaluated by using the American Society for Testing and Materials (ASTM) methods. To ensure the accuracy of measurements, each sample was analyzed in triplicate.

For ash analysis, porcelain crucibles were preheated in an oven at 650 °C for 10 min; next, the crucibles were cooled in a desiccator at room temperature and preweighed. The ash content was determined by measuring the mass loss after the combustion of 1 g of biochar sample in the porcelain crucible at 105 °C for 1 h and 750 °C for 6 h (ASTM, 2018a).

The VM content was determined by heating the dried sample at 900 °C in a muffle furnace (SP-1200DM/B, Splabor, Presidente Prudente, São Paulo, Brazil). Approximately 1 g of dried biochar sample was weighed and placed in a preweighed and preheated porcelain crucible. The crucible was placed in the preheated muffle door at 900 °C for 3 min and then placed inside the muffle furnace for 7 min. After the oven cooled, the samples were removed and placed in a desiccator at room temperature and then weighed. The VM content was determined by the mass difference in the crucible before being placed in the muffle furnace and after being removed from the muffle furnace (ASTM, 2018b).

2.2.3 pH value and electrical conductivity (EC)

For pH measurements, 2 g of each biochar sample was weighed into a 25 mL beaker; next, 10 mL of a 0,01 M $CaCl_2$ was added to the beaker and stirred with a glass rod; and then, the mixture was allowed to sit for 1 h (ISO, 2005). The pH measurement was performed with a digital pH meter (Mpa-210, Tecnopon, Piracicaba, São Paulo, Brasil).

The electrical conductivity (EC) was determined by the BGK method (FCQAO, 1994). A solution of 2 g of dry biochar and 10 mL of deionized water was prepared and stirred for 1 h. Then, the measurements were performed on a digital conductivity meter (MA 521, Marconi, Piracicaba, São Paulo, Brasil). The pH and EC analyses were performed in duplicate.

2.2.4 Specific surface area (SSA) and morphology

Scanning electron microscopy (SEM) was used to evaluate the changes in the physical morphology of the biochar surface caused by variations in pyrolysis temperature. The biochar particles were placed in a metal sample holder using carbon conductive tape (PELCO Tabs™, Ted Pella, Inc., Redding, CA, EUA) and sputtered (Q150R ES, Quorum Technologies Ltd., Laughton, East Sussex, England) with a 9-nm thick gold layer. This procedure is used to improve material conductivity, generating a higher quality image. Images were captured with

a secondary electron detector (SE) in SEM (VEGA 3 LMU, Tescan, República Tcheca), operating with an electron beam of 20 kV.

The textural properties of the biochar surface were characterized with the Brunauer-Emmett-Teller (BET) method by using results from the physical adsorption of N_2 at 77 K with the aid of a surface area analyzer (ASAP-2020, Micromeritics, Norcross, GA, EUA), with a relative pressure range (P/P_0) of 0,01 to 0,99. At each pressure, the physically adsorbed N_2 produces a change in the output composition, which is recorded by a thermal conductivity detector that is connected to a potentiometric recorder. By heating the sample, there is a loss in contact of the liquid N_2 with the sample, and the N_2 is desorbed. The peak area is proportional to the mass of desorbed N_2. From the N_2 volume obtained in the assay and using the BET equation, the specific surface area (SSA) and total pore volume (TPV) were determined.

2.2.5 Chemical analysis

The spatial arrangements and presence of minerals in the samples were identified using the X-ray diffraction (XRD) technique; the bands were scanned in the 2θ range from 10-80° at low and medium angles (XRD 6000, Shimadzu, Quioto, Japão) with a radiation source of CuKα (λ = 0,15406 nm), a nickel filter operating at 30 kV and a rate of 30 mA at 0,6°/min.

The surface functional groups were analyzed by Fourier transform infrared spectroscopy (FT-IR) in the wavelength range of 400-4000 cm^{-1} (by 64 scans with 4 cm^{-1} resolution). Before FTIR analysis, the samples were oven dried at 200 °C, and then 0.5 mg of the sample was mixed with 300 mg of KBr and ground. Shortly after, each sample was pressed in a hydraulic press (Shimadzu, SSP-10A, Tokyo, Japan) at 80 kN force to form a tablet that was analyzed on a spectrometer (IRPrestige-21, Shimadzu, Tokyo, Japão).

Due to the need for a relative scale of the absorption intensity, a background spectrum was measured, which consisted of comparing a sample-free beam measurement to the sample-beam measurement to determine the percent transmittance. All spectral information was strictly due to the sample. As the background spectrum is a feature of the instrument, only one measurement of this spectrum was performed.

2.3 Data analysis

The degree of linear association between two measured variables was analyzed using the Pearson correlation coefficient. The relationships between pyrolysis conditions (independent variables) and biochar-derived properties (dependent variables) were evaluated.

A significance rate was considered ($p \leq 0.05$). R values were calculated using Statistica® software version 7.0 (StatSoft Company, EUA).

3 RESULTS AND DISCUSSION

3.1 Effect of pyrolysis temperature on yield, VM content, ash content, pH value, EC and inorganic minerals from biochar produced

A significant negative correlation occurred between the pyrolysis temperature and charcoal yield (R= -0,90), indicating a decrease in yield due to the increased pyrolysis temperature (Table 1). The yield declined sharply as the temperature increased from 450 to 650 °C (Table 1). The volatile matter content showed a similar behavior to yield, and there was an exponential reduction in volatile matter content from 450 to 650 °C and a significant correlation of -0.90 (Table 1). The main transformation observed over this temperature range is the thermal decomposition of lignocellulosic materials and the release of water vapor and volatile matter compounds such as CO, CO_2, H_2, and CH_4, resulting in a high yield loss at lower temperatures (LIU et al., 2015; LI; CHEN, 2018; YANG et al., 2019). Between 750 and 850 °C, the decline in biochar yield was proportionally lower and constant, indicating the formation of the most stable carbonaceous compound in terms of material loss. Other studies have shown a similar correlation for other materials reacted at different pyrolysis temperatures; that is, other materials show a rapid initial decline in yield at lower temperatures, followed by a smaller and constant reduction at higher temperatures (KEILUWEIT et al., 2010; XIAO et al., 2014; YUAN et al., 2015; WEI et al., 2019).

Table 1. Yield, ash, volatile matter (VM) contents, pH and electrical conductivity (EC) of pyrolyzed eucalyptus wood-derived biochar at different temperatures.

Temperature	Yield	Ash	(VM)	pH	EC
(°C)		(%)		($CaCl_2$)	µS/cm
450	42.76	0.60	30.32	5.3	123.3
550	38.00	0.74	16.49	6.7	97.4
650	34.69	0.63	11.92	9.7	134.3
750	34.27	0.84	5.52	9.8	164.6
850	32.44	0.82	3.43	9.1	161.6
950	33.47	1.06	3.63	9.2	273.1
Correlations	-0.90*	0.89*	-0.90*	0.83*	0.85*

* Significant correlations ($p \leq 0,05$).

Unlike yield and VM content, the ash content, pH value and EC increased due to the temperature increase, with significant positive correlations of 0.89, 0.83 and 0.85, respectively (Table 1). The higher ash content observed at higher temperatures is caused by the stability of minerals in the pyrolyzed product, such as K, Ca and P, following a progressive loss in volatile matter from the devolatilization process (WEBER; QUICKER, 2018). This observation was explained by the positive correlation of these minerals with the temperature increase (Table 2). Another observed effect associated with higher ash content is the increase in pH value and EC. Lehmann and Joseph (2015) developed a meta-analysis and reported a close relationship between pyrolysis temperature and pH value. These authors observed that the average pH value of pyrolyzed biochar was 5 at <400 °C, while the pH value of pyrolyzed biochar was 9 at > 600 °C. The ability of biochar to neutralize the acidity has been acknowledged in several studies, showing biochar to be a potential agent for correcting the pH value in acidic soils, reducing the toxicity of aluminum and increasing the availability of nutrients (JEFFERY et al., 2011; BUTNAN et al., 2015; ZHAO et al., 2015; BURRELL et al., 2016; TEUTSCHEROVA et al., 2017).

Table 2. Eucalyptus wood-derived biochar inorganic minerals produced at different pyrolysis temperatures.

Temperature (°C)	K	Ca	P	Fe	S (%)	Mn	Zn	Cr	Si
450	0.182	0.085	0.016	0.001	0.014	0.002	----	----	----
550	0.140	0.104	0.016	0.003	0.013	0.003	----	----	0.045
650	0.164	0.115	0.023	0.006	0.016	0.003	0.0002	0.002	----
750	0.210	0.130	0.017	0.006	0.010	0.003	----	----	----
850	0.210	0.104	0.025	0.004	0.016	0.002	----	----	----
950	0.286	0.176	0.031	0.004	0.013	0.003	----	----	----
Correlations	0.82*	0.82*	0.84*	0.51	-0.05	0.21			

* Significant correlations ($p \leq 0.05$).

In addition to the pH value, the increase in cation concentrations due to the increase in the pyrolysis temperature favored the higher EC of the material. Biochars with the highest concentration of salts can be a problem in areas with the limited ability to leach salts. The constant application of biochar with high EC values can reduce seed germination and crop yields with higher sensitivity to salt in the soil solution (PAZ-FERREIRO et al., 2018). However, most studies showed a positive correlation effect between biochar use and lower crop toxicity due to water and saline stress (BOUQBIS et al., 2017; OLSZYK et al., 2018; MUMME et al., 2018; MEHDIZADEH et al., 2019). The increase in biochar EC due to a higher pyrolysis temperature is mainly caused by the higher K concentration as observed in this work (Table 2).

The K supply via the biochar application can improve osmotic control and the potassium/sodium ratio, which increases the crop tolerance to water and saline stress (REZAIE et al., 2019).

3.2 Elemental Analysis

The pyrolysis temperature changed the elemental composition of the eucalyptus wood waste-derived biochar (Table 3). Increasing the temperature from 450 to 950 °C increased the C content from 74.96% to 86.93%, respectively, with a significant positive correlation (R = 0.84) (Table 2). The H and O content were negatively correlated with the increase in pyrolysis temperature (R = 0.72 and 0.84, respectively), with a decrease of 3.76% to 0.9% in H content and 19.41% to 10.75% in O content. The gradual increase in C content of the biochar due to the increase in temperature is caused by a higher release rate of hydrogen and oxygen in the form of water vapor (dehydration) and the loss of functional groups associated with these atoms (carboxyl groups and hydroxyls). During the carbonization process, the relative loss in hydrogen and oxygen is higher than the relative loss in carbon (WEBER; QUICKER, 2018); this behavior was also observed for the eucalyptus-derived biochar, changing the atomic ratios of biochars.

Table 3. Elemental analysis, specific surface area and total pore volume of pyrolyzed eucalyptus wood biochar at different temperatures.

Temperature	Elemental Analysis							Surface specific area and total pore volume	
(°C)	C %	H %	O %	N %	H/C	O/C	(O+N)/C	SSA (m^2 g^{-1})	TPV (mm^3 g^{-1})
450	74.96	3.76	19.41	1.25	0.050	0.25	0.27	-	-
550	79.25	1.00	18.01	1.49	0.012	0.22	0.25	-	-
650	87.06	1.60	10.70	0.00	0.018	0.12	0.12	410.48	0.05
750	87.74	0.87	9.47	1.06	0.019	0.11	0.12	402.51	0.07
850	88.01	0.89	8.99	1.27	0.010	0.10	0.14	362.90	0.08
950	86.90	0.90	10.57	1.34	0.002	0.12	0.17	224.43	0.02
Correlation	0.84*	0.72	0.84*	0.08	-0.80	0.85*	-0.81	-0.89*	-0.34

Hydrogen potential (pH value), electrical conductivity (EC), elemental carbon (C), elemental hydrogen (H), elemental oxygen (O), elemental nitrogen (N), aromaticity index (H/C), hydrophilicity index (O/C), polarity index (O + N)/C, surface specific area (SSA) and total micropore volume (TMV) of the biochar by pyrolysis temperature. * Significant correlations ($p \leq 0.05$).

The O/C ratio had a significant negative correlation with the increase in temperature (R = -0.85) (Table 3). The correlation with the H/C and (O + N)/C ratios was not significant, although the correlation showed high values (R = -0.8 and -0.81, respectively) (Table 2). The

reduction in atomic ratios due to the increased temperature pyrolysis indicates that the material formed has a higher aromaticity and recalcitrance but a smaller polarity (KEILUWEIT et al., 2010, USMAN et al., 2015, ZHAO et al., 2018). These properties ensure that biochar has a greater resistance to degradation when applied to soils (SPOKAS et al., 2010; HUANG et al., 2017, LI et al., 2019). For the biochar derived from eucalyptus produced at 850 and 950 °C, the increased stability of these carbonaceous materials can provide carbon sequestration in soil since they are hardly changed in their elemental structure. Despite the lower H/C and O/C ratios of biochars produced at pyrolysis temperatures of 850 and 950 °C, all other biochars produced at the lowest temperatures in this research are within the parameters required by the European Biochar Certificate (EBC, 2012): C%> 50, H/C ratio <0.7 and O/C ratio <0.4.

The pyrolysis temperature did not change the N content, showing a nonsignificant correlation (R = 0.08) (Table 3). Generally, the N content depends on the type of raw material used for biochar production and not on the pyrolysis conditions (ZHANG et al., 2015; ZHAO et al., 2018). Moreover, in woody matrices, N-containing structures are more resistant to degradation with increasing temperature. According to Enders et al. (2012), N is highly retained in raw material wood-derived biochars, which is probably due to the formation of heterocyclic N such as pyridines and pyrroles.

The van Krevelen diagram allows us to identify changes in the H/C and O/C ratios in eucalyptus-derived biochar (Figure 1). An increase in the pyrolysis temperature from 450 to 550 °C promoted an intense reduction in aliphatic groups (H/C). At temperatures above 550 °C, the aliphatic degree of biochar changed little. The main change from 550 °C was the reduction in the O/C ratio, providing biochar with a greater similarity for the H/C and O/C ratios. Pyrolysis at 950 °C promoted another decrease in the H/C ratio. This behavior observed for the higher pyrolysis temperatures suggests the beginning of the formation process of a carbonaceous material with a high amount of metamorphism called coal anthracite (HAYKIRI-ACMA; YAMAN, 2010).

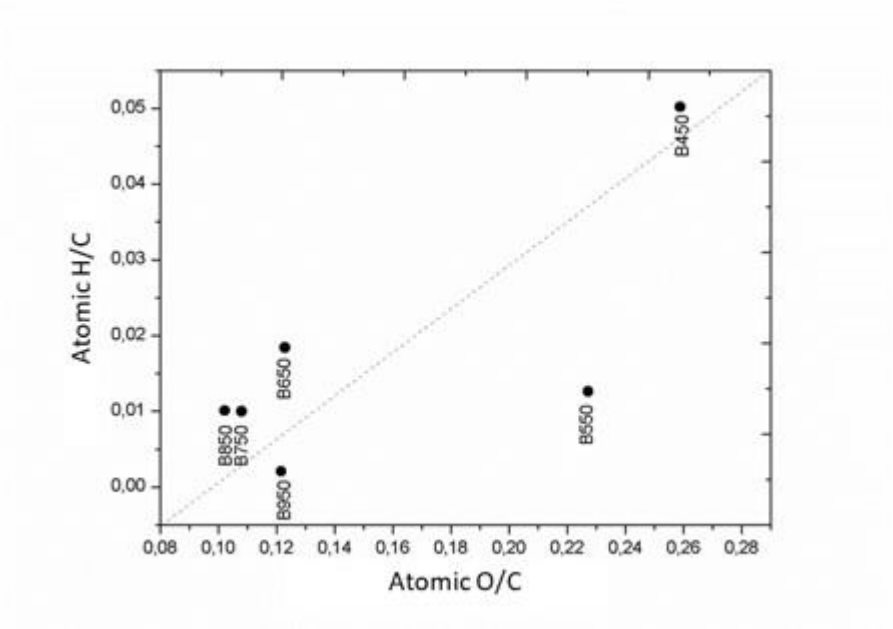

Figure 1. Van Krevelen diagram, correlation between H/C and O/C ratios of pyrolyzed eucalyptus wood-derived biochar at different temperatures.

3.3 Specific surface area and total pore volume, surface morphology, crystalline phase and functional groups

The pyrolysis temperature showed a significant negative correlation with the biochar specific surface area (R = -0.89) (Table 3). As the pyrolysis temperature increased from 650 to 950 °C, the SSA decreased from 410.48 to 224.43 m^2 g^{-1}, respectively. This reduction in the SSA due to material burning at higher temperatures is not common. Most studies show that a higher pyrolysis temperature provides a higher SSA (SUN et al., 2014; ZHAO et al., 2018). For eucalyptus-derived biochar, the reduction in the SSA can be attributed to the higher ash content observed at temperatures above 650 °C (Table 1), which can decrease the formation of the microporous structure (LIU et al., 2014). In addition, micropores can be destroyed by the polymerization reaction during the heating process (NEVES et al., 2011), resulting in a lower SSA found in biochar produced at higher pyrolysis temperatures.

The increased pyrolysis temperature showed no significant correlation with the TPV (R = -0,34). The TPV increased from 0.05 to 0.07 mm^3 g^{-1} from 650 to 850 °C, respectively, and decreased to 0.02 mm3 g^{-1} at 950 °C. Increasing the temperature to 950 °C may have destroyed or blocked the micropores. Moreover, the XRD analysis results show that the microcrystalline graphite structure is more present in high-temperature biochars (Figure 3). The process of converting amorphous carbon into graphite microcrystalline structures can cause a decrease in the TPV and SSA, as reported by Chen et al. (2012) when evaluating the effect of pyrolysis temperature on cotton stalks. At temperatures of 450 and 550 °C, the device could not

determine the SSA and TPV. The amount of uncarbonized biomass at these temperatures may have interfered with the measurements, and this prevents the gas adsorption measurements (N_2-BET), which allow for the estimation of the surface area and pore volume (ESSANDOH et al., 2015 e 2017).

The SEM images at 200x and 1000x magnification show that increasing the pyrolysis temperature promoted the loss of the outer biochar layer (Figure 2). Removal of the outer biochar layer exposes pores located in the carbonaceous skeleton of the biological capillary structure of the raw material. A greater number of porous structures was observed with increasing pyrolysis temperature (Figure 2). However, the accumulation of particles on the biochar surface, mainly ash, was also increased due to the higher temperature used (Figure 2). The presence of this greater amount of ash on the surface of biochars produced at higher temperatures justifies the evidence that these particles could clog the micropores, reducing both the SSA and TPV measured during the BET analysis.

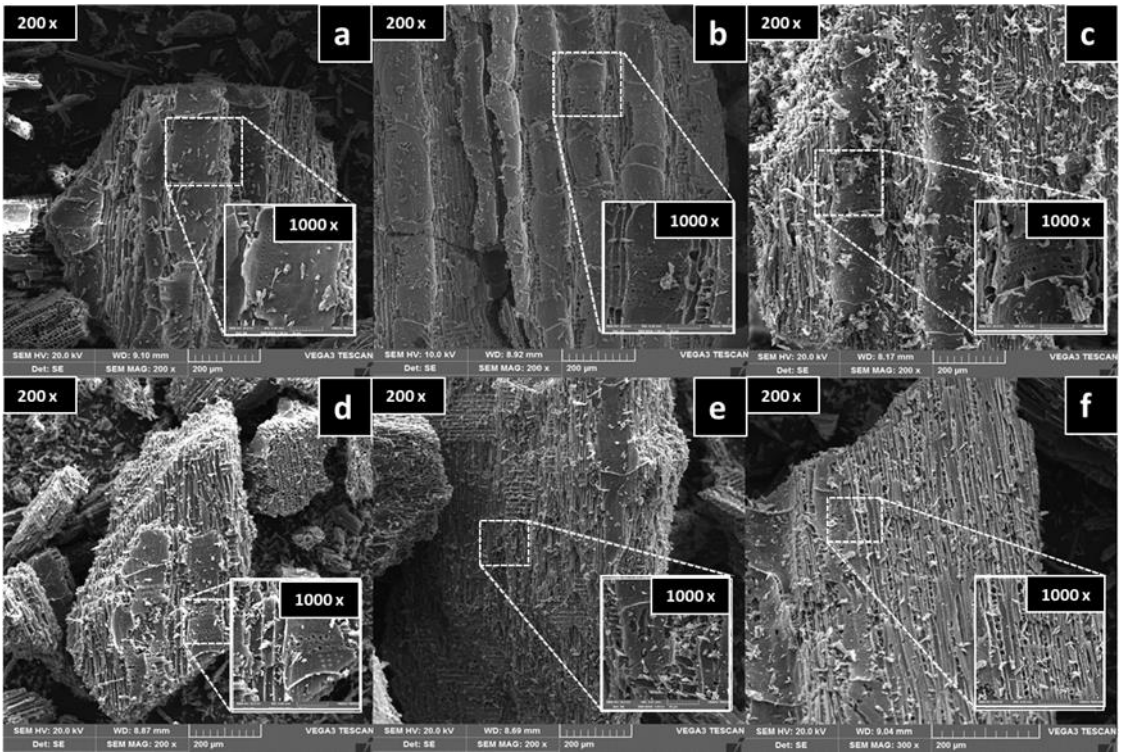

Figure 2. Scanning electron microscopy (SEM) of eucalyptus wood-derived biochar produced at different pyrolysis temperatures at 200 and 1000x magnification: (a) 450 (b) 550 (c) 650 (d) 750 (e) 850 and (f) 950 °C.

The crystalline phase shape and biochar purity were determined using XRD analysis. The spectrum showed that there were no sharp peaks that represent the presence of crystalline mineral structures (Figure 3). The XRD peak intensities increased with increasing pyrolysis

temperature. The 2θ angle peak at approximately 22.7° is attributed to the crystallographic planes hkl 101 of the crystalline regions of cellulose (JIANG et al., 2007; BISWAS et al., 2017). Pyrolysis temperatures above 650 °C resulted in a wider peak at 2θ value of approximately 23.5°, indicating that some partial crystalline structure of the cellulose was lost (KEILUWEIT et al., 2010). A new 2θ peak of approximately 43.7° became clearer in biochars at pyrolysis temperatures of 750 to 950 °C. This new observed peak indicates the development of graphite-like atomic order in the increasingly charred material (KEILUWEIT et al., 2010). This peak results in the successive ordering of carbon in aromatic structures (PARIS et al., 2005), indicating the highest crystallization of the carbonaceous material (TUSHAR et al., 2012). These findings point to the formation of more stable (less reactive) graphitic carbon at higher pyrolysis temperatures.

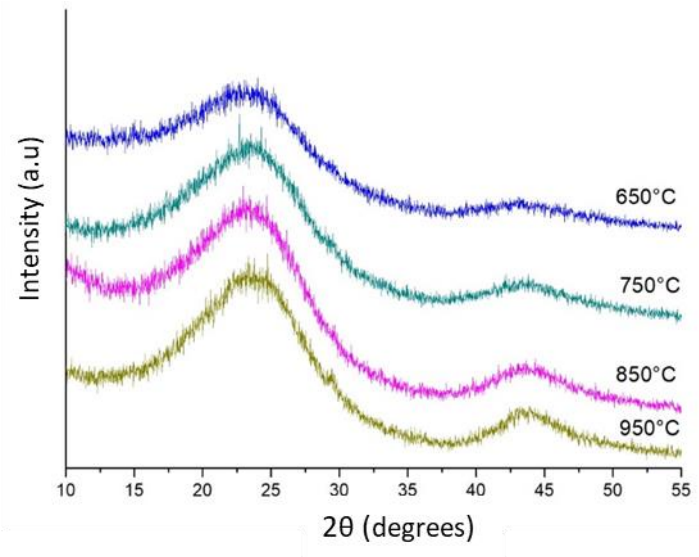

Figure 3. X-ray diffractometers, diffracted beam intensity as a function of Bragg angle (2θ in degrees) of eucalyptus wood-derived biochar at different pyrolysis temperatures.

The functional groups observed in the eucalyptus wood residue-derived biochar by FT-IR analysis are listed in Table 4. Aromatic, aliphatic and phenolic groups were seen as the predominant peaks. A high intensity peak at 3.424 cm^{-1}, corresponding to the stretching vibrations of the –OH groups, became weaker with increasing temperature (Table 3 and Figure 4). There was a reduction in peaks from 1000-1700 cm^{-1} with increasing pyrolysis temperature (Figure 4). At lower temperatures (450, 550 and 650 °C), peaks at 1.604 cm^{-1} (C = O) (UCHIMIYA et al., 2011) and 1.240 cm^{-1} (C-O acetyls) are observed, suggesting the presence of woody and cellulosic constituents and the incomplete degradation of the original biomass (AL-WABEL et al., 2013).

The peak at 2.920 cm^{-1} (C-H, CH_2 or CH_3) (BISWAS et al., 2017) for aliphatic components was observed only at lower temperatures (450 and 550 °C) (Figure 3). With increasing pyrolysis temperature > 550 °C, the aliphatic C-H stretching observed at a peak of 2.920 cm^{-1} was completely eliminated, suggesting the degradation of hemicellulose and cellulose (USMAN et al., 2015). The peak representing the aromatic carbon at 1.638 cm^{-1} (C=C) (CHEN, 2008; BISWAS et al., 2017) narrowed at the temperature of 750 °C (Table 4 and Figure 4). The higher peak intensity for the C = C group confirms the increased aromaticity of the eucalyptus-derived biochar when produced at temperatures above 750 °C. The peak intensity at 1.430 cm-1 for C-H decreased dramatically with increasing temperature, reaching close to zero intensities when the material was pyrolyzed at 950 °C.

Table 4. Absorption peak intensity by wavelength and pyrolysis temperature of eucalyptus wood biochar

FT-IR Peak (cm^{-1})	Pyrolysis Temperature (°C)						Vibration	References
	450	550	650	750	850	950		
3.424	Strong	Medium	Weak	Medium	Medium	Weak	O-H Alcohol or phenol	CHEN et al., 2008
2.920	Weak	Weak	-	-	-	-	CH_2-CH_3 Aliphatic	BISWAS et al., 2017
1.638	Weak	Weak	Medium	Strong	Strong	Strong	C=C	BISWAS et al, 2017
1.604	Medium	Medium	Weak	-	-	-	C=O/C=C Aromatics, ketones	UCHIMIYA et al., 2011
1.430	Strong	Strong	Weak	Weak	Weak	Weak	C-H carboxymethyl-cellulose	ADEL et al., 2010
870	Weak	Weak	Strong	Weak	Weak	Weak	C-H in polycyclic aromatic	MARX et al., 2014

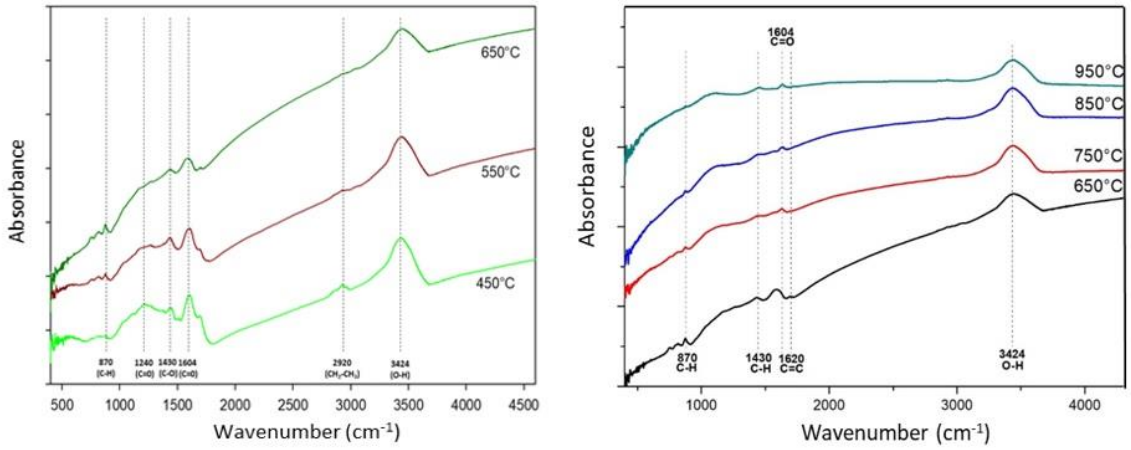

Figure 4. Infrared spectra (FT-IR) of eucalyptus wood-derived biochar samples at different pyrolysis temperatures.

Increasing the pyrolysis temperature reduced the intensity of some biochar functional groups. This loss of functional groups, especially the hydroxyl and carboxyl groups, is caused by the degradation and transformation of hemicellulose (200-260 °C), cellulose (315-400 °C) and lignin (> 400 °C) in homogeneous and highly aromatic carbon structures (YANG, 2018). The FT-IR spectra confirm the transformation of the eucalyptus-derived material into more recalcitrant compounds when high pyrolysis temperatures are used during biochar synthesis. However, the absence of functional groups (carboxylic, phenolic and alcohols) can make it impossible to use biochar for some specific purposes. The application of highly aromatic biochar without functional groups to reduce nutrient leaching (DELUCA et al., 2015) or to remove soil contaminants (YUAN et al., 2018) can be inefficient due to the absence of surface charges that are capable of interacting with nutrients or contaminants.

4 CONCLUSIONS

Some physicochemical properties of eucalyptus wood-derived biochar are affected by pyrolysis temperature. The results show that the pyrolysis temperature is positively correlated with pH value, electrical conductivity, ash content and elemental carbon and negatively correlated with yield, volatile matter, elemental oxygen, elemental hydrogen, surface area and H/C, O/C and (O + N)/C ratios. An increase in temperature promoted a loss in biochar surface layers, reduction in surface functional groups and formation of a more stable carbon. Overall, the research indicates that the pyrolysis temperature makes it possible to produce biochar from the same raw material with a wide range of physicochemical properties, allowing its use in various types of agricultural and environmental activities, such as soil conditioning, carbon sequestration or the immobilization of contaminants.

REFERENCES

ADEL, A. M. et al. Characterization of microcrystalline cellulose prepared from lignocellulosic materials. Part I. Acid catalyzed hydrolysis. **Bioresource Technology**, v. 101, n. 12, p. 4446-4455, 2010.

AL-WABEL, M. I. et al. Pyrolysis temperature induced changes in characteristics and chemical composition of biochar produced from conocarpus wastes. **Bioresource Technology**, v. 131, p. 374-379, 2013.

ASTM. American Society for Testing and Materials, **Standard Test Method for Ash in the Analysis Sample of Coal and Coke from Coal**. D3174 – 12 (2018). Disponível em: <https://compass.astm.org/EDIT/html_annot.cgi?D3174+12(2018)>. Acesso em: 12 de out. de 2019.

ASTM. American Society for Testing and Materials, **Standard Test Method for Volatile Matter in the Analysis Sample of Coal and Coke**. D3175 (2018). Disponível em: <https://compass.astm.org/EDIT/html_annot.cgi?D3175+18>. Acesso em: 12 de out. de 2019.

AWASTHI, M. K. et al. Effect of biochar amendment on greenhouse gas emission and bio-availability of heavy metals during sewage sludge co-composting. **Journal of Cleaner Production**, v. 135, p. 829-835, 2016.

BGK **Methodenbuch zur Analyse von Kompost (BGK e.V.) [Methods Book for the Analysis of Compost, Federal Compost Quality Assurance Organisation (BGK e.V.)]**Abfall Now (Hrsg.), Stuttgart, 1994.

BISWAS, B. et al. Pyrolysis of agricultural biomass residues: Comparative study of corn cob, wheat straw, rice straw and rice husk. **Bioresource Technology**, v. 237, p. 57-63, 2017.

BOUQBIS, L. et al. Phytotoxic effects of argan shell biochar on salad and barley germination. **Agriculture and Natural Resources**, v. 51, n. 4, p. 247-252, 2017.

BURRELL, L. D. et al. Long-term effects of biochar on soil physical properties. **Geoderma**, v. 282, p. 96-102, 2016.

BUTNAN, S. et al. Biochar characteristics and application rates affecting corn growth and properties of soils contrasting in texture and mineralogy. **Geoderma**, v. 237, p. 105-116, 2015.

CAO, X. et al. Comparative study of the pyrolysis of lignocellulose and its major components: Characterization and overall distribution of their biochars and volatiles. **Bioresource Technology**, v. 155, p. 21-27, 2014.

CHEN, B. et al. Transitional adsorption and partition of nonpolar and polar aromatic contaminants by biochars of pine needles with different pyrolytic temperatures. **Environmental Science & Technology**, v. 42, n. 14, p. 5137-5143, 2008.

CHEN, D. et al. Bamboo pyrolysis using TG–FTIR and a lab-scale reactor: Analysis of pyrolysis behavior, product properties, and carbon and energy yields. **Fuel**, v. 148, p. 79-86, 2015.

CHEN, Y. et al. Biomass-based pyrolytic polygeneration system on cotton stalk pyrolysis: influence of temperature. **Bioresource Technology**, v. 107, p. 411-418, 2012.

DELUCA, T. H. et al. Biochar effects on soil nutrient transformations. In: LEHMAN, J.; JOSEPH, S. (Ed.) **Biochar for Environmental Management: science, technology and implementation**, New York: Routledge, 2015, p. 421-454.

EBC, IBI. Comparison of European Biochar Certificate Version 4. 8 and IBI Biochar Standards Version 2.0 **IBI Biochar Stand. first Publ**. European Biochar Certificate first publication March 2012. p. 1-5. Disponível em: <http:// www.european-biochar.org/en/home>. Acesso em: 02 de Out. de 2019

ELKHALIFA, S. et al. Food waste to biochars through pyrolysis: A review. **Resources, Conservation and Recycling**, v. 144, p. 310-320, 2019.

ENDERS, A. et al. Characterization of biochars to evaluate recalcitrance and agronomic performance. **Bioresource Technology**, v. 114, p. 644-653, 2012.

ESSANDOH, M. et al. Phenoxy herbicide removal from aqueous solutions using fast pyrolysis switchgrass biochar. **Chemosphere**, v. 174, p. 49-57, 2017.

ESSANDOH, M. et al. Sorptive removal of salicylic acid and ibuprofen from aqueous solutions using pine wood fast pyrolysis biochar. **Chemical Engineering Journal**, v. 265, p. 219-227, 2015.

GAO, S. et al. Locally produced wood biochar increases nutrient retention and availability in agricultural soils of the San Juan Islands, USA. **Agriculture, Ecosystems & Environment**, v. 233, p. 43-54, 2016.

HAYKIRI-ACMA, H.; YAMAN, S. Interaction between biomass and different rank coals during co-pyrolysis. **Renewable Energy**, v. 35, n. 1, p. 288-292, 2010.

HUANG, H. J. et al. Co-pyrolysis of sewage sludge and sawdust/rice straw for the production of biochar. **Journal of Analytical and Applied Pyrolysis**, v. 125, p. 61-68, 2017.

HUFF, M. D. et al. Comparative analysis of pinewood, peanut shell, and bamboo biomass derived biochars produced via hydrothermal conversion and pyrolysis. **Journal of Environmental Management**, v. 146, p. 303-308, 2014.

IBÁ. Indústria Brasileira de Árvores (Brazilian Tree Industry). **Annual report 2017.** IBÁ, São Paulo, Brazil. 2017.

IPEA. Instituto de Pesquisas Aplicadas Diagnóstico dos Resíduos Orgânicos do Setor Agrossilvopastoril e Agroindústrias Associadas: **Relatório de Pesquisa.** Governo Federal. Brasília. 2012. Disponível em: <http://www.ipea.gov.br/portal/images/stories/PDFs/relatoriopesquisa/120917_relatorio_residuos_organicos.pdf>. Acesso em: 18 de Out. de 2019.

ISO. International Standards Organization. **Soil Quality–Determination of pH (ISO 10390: 2005).** Disponível em:< https://www.iso.org/standard/40879.html>. Acesso em: 12 de Out. de 2019.

JEFFERY, S. et al. A quantitative review of the effects of biochar application to soils on crop productivity using meta-analysis. **Agriculture, Ecosystems & Environment**, v. 144, n. 1, p. 175-187, 2011.

JIANG, Z. H. et al. Rapid prediction of wood crystallinity in *Pinus elliotii* plantation wood by near-infrared spectroscopy. **Journal of Wood Science**, v. 53, n. 5, p. 449-453, 2007.

JONES, D. L.; EDWARDS-JONES, G.; MURPHY, D. V. Biochar mediated alterations in herbicide breakdown and leaching in soil. **Soil Biology and Biochemistry**, v. 43, n. 4, p. 804-813, 2011.

JUNNA, S. et al. Effects of wheat straw biochar on carbon mineralization and guidance for large-scale soil quality improvement in the coastal wetland. **Ecological Engineering**, v. 62, p. 43-47, 2014.

KEILUWEIT, M. et al. Dynamic molecular structure of plant biomass-derived black carbon (biochar). **Environmental Science & Technology**, v. 44, n. 4, p. 1247-1253, 2010.

KOOKANA, R. S. et al. Biochar application to soil: agronomic and environmental benefits and unintended consequences. **Advances in Agronomy**, v. 112, p. 103-143, 2011.

LEHMANN, J.; JOSEPH, S. Biochar for environmental management: an introduction. In: **Biochar for Environmental Management**. Routledge, 2015. p. 33-46.

LI, S.; CHEN, G. Thermogravimetric, thermochemical, and infrared spectral characterization of feedstocks and biochar derived at different pyrolysis temperatures. **Waste Management**, v. 78, p. 198-207, 2018.

LI, S. et al. Predicting biochar properties and functions based on feedstock and pyrolysis temperature: A review and data syntheses. **Journal of Cleaner Production**, v. 215, p. 890-902, 2019.

LIN, Q. et al. The speciation, leachability and bioaccessibility of Cu and Zn in animal manure-derived biochar: effect of feedstock and pyrolysis temperature. **Frontiers of Environmental Science & Engineering**, v. 11, n. 3, p. 5-17, 2017.

LIU, W. J. et al. Development of biochar-based functional materials: toward a sustainable platform carbon material. **Chemical Reviews**, v. 115, n. 22, p. 12251-12285, 2015.

LIU, X. et al. Characterization of corncob-derived biochar and pyrolysis kinetics in comparison with corn stalk and sawdust. **Bioresource technology**, v. 170, p. 76-82, 2014.

MANNA, S.; SINGH, N. Biochars mediated degradation, leaching and bioavailability of pyrazosulfuron-ethyl in a sandy loam soil. **Geoderma**, v. 334, p. 63-71, 2019.

MARX, S. et al. Influence of reaction atmosphere and solvent on biochar yield and characteristics. **Bioresource Technology**, v. 164, p. 177-183, 2014.

MEHDIZADEH, L.; MOGHADDAM, M.; LAKZIAN, A. Alleviating negative effects of salinity stress in summer savory (*Satureja hortensis* L.) by biochar application. **Acta Physiologiae Plantarum**, v. 41, n. 6, p. 98, 2019.

MENDES, K. F. et al. Cow bone char as a sorbent to increase sorption and decrease mobility of hexazinone, metribuzin, and quinclorac in soil**. Geoderma**, v. 343, p. 40-49, 2019.

MUMME, J. et al. Toxicity screening of biochar-mineral composites using germination tests. **Chemosphere**, v. 207, p. 91-100, 2018.

NEVES, D. et al. Characterization and prediction of biomass pyrolysis products. **Progress in Energy and Combustion Science,** v. 37, n. 5, p. 611-630, 2011.

OLSZYK, D. M. et al. A rapid-test for screening biochar effects on seed germination. **Communications in Soil Science and Plant Analysis**, v. 49, n. 16, p. 2025-2041, 2018.

PARIS, O. Decomposition and carbonisation of wood biopolymers-a microstructural study of softwood pyrolysis. **Carbon**, v. 43, n. 1, p. 53-66, 2005.

PAZ-FERREIRO, J. et al. Biochar from biosolids pyrolysis: a review. **International Journal of Environmental Research and Public Health**, v. 15, n. 5, p. 956-972, 2018.

REZAIE, N.; RAZZAGHI, F.; SEPASKHAH, A. R. Different levels of irrigation water salinity and biochar influence on faba bean yield, water productivity, and ions uptake. **Communications in Soil Science and Plant Analysis**, v. 50, n. 5, p. 611-626, 2019.

RONSSE, F. et al. Production and characterization of slow pyrolysis biochar: influence of feedstock type and pyrolysis conditions. **Gcb Bioenergy**, v. 5, n. 2, p. 104-115, 2013.

SINGH, R. et al. Multifaceted application of crop residue biochar as a tool for sustainable agriculture: an ecological perspective. **Ecological Engineering**, v. 77, p. 324-347, 2015.

SPOKAS, K. A. et al. Biochar: a synthesis of its agronomic impact beyond carbon sequestration. **Journal of Environmental Quality**, v. 41, n. 4, p. 973-989, 2012.

SPOKAS, K. A. Review of the stability of biochar in soils: predictability of O: C molar ratios. **Carbon Management**, v. 1, n. 2, p. 289-303, 2010.

SRINIVASAN, P.; SARMAH, A. K. Characterization of agricultural waste-derived biochars and their sorption potential for sulfamethoxazole in pasture soil: a spectroscopic investigation. **Science of the Total Environment**, v. 502, p. 471-480, 2015.

SULIMAN, W. et al. Influence of feedstock source and pyrolysis temperature on biochar bulk and surface properties. **Biomass and Bioenergy**, v. 84, p. 37-48, 2016.

SUN, Y. et al. Effects of feedstock type, production method, and pyrolysis temperature on biochar and hydrochar properties. **Chemical Engineering Journal**, v. 240, p. 574-578, 2014.

TEUTSCHEROVA, N. et al. Comparison of lime-and biochar-mediated pH changes in nitrification and ammonia oxidizers in degraded acid soil. **Biology and Fertility of Soils**, v. 53, n. 7, p. 811-821, 2017.

TRIPATHI, M. et al. Effect of process parameters on production of biochar from biomass waste through pyrolysis: a review. **Renewable and Sustainable Energy Reviews**, v. 55, p. 467-481, 2016.

TUSHAR, M. S. H. K. et al. Production, characterization and reactivity studies of chars produced by the isothermal pyrolysis of flax straw. **Biomass and Bioenergy**, v. 37, p. 97-105, 2012.

UCHIMIYA, M. et al. Influence of pyrolysis temperature on biochar property and function as a heavy metal sorbent in soil. **Journal of Agricultural and Food Chemistry**, v. 59, n. 6, p. 2501-2510, 2011.

USMAN, A. R. A. et al. Biochar production from date palm waste: charring temperature induced changes in composition and surface chemistry. **Journal of Analytical and Applied Pyrolysis**, v. 115, p. 392-400, 2015.

WEBER, K.; QUICKER, P. Properties of biochar. **Fuel**, v. 217, p. 240-261, 2018.

WEI, S. et al. Influence of pyrolysis temperature and feedstock on carbon fractions of biochar produced from pyrolysis of rice straw, pine wood, pig manure and sewage sludge. **Chemosphere**, v. 218, p. 624-631, 2019.

XIAO, X. et al. Transformation, morphology, and dissolution of silicon and carbon in rice straw-derived biochars under different pyrolytic temperatures. **Environmental Science & Technology**, v. 48, n. 6, p. 3411-3419, 2014.

YANG, F. et al. Effective sorption of atrazine by biochar colloids and residues derived from different pyrolysis temperatures. **Environmental Science and Pollution Research**, v. 25, p. 18528-18539, 2018.

YANG, X. et al. Characterization and ecotoxicological investigation of biochar produced via slow pyrolysis: Effect of feedstock composition and pyrolysis conditions. **Journal of Hazardous Materials**, v. 365, p. 178-185, 2019.

YANG, X. et al. Effect of biochar on the extractability of heavy metals (Cd, Cu, Pb, and Zn) and enzyme activity in soil. **Environmental Science and Pollution Research**, v. 23, n. 2, p. 974-984, 2016.

YUAN, H. et al. Influence of pyrolysis temperature on physical and chemical properties of biochar made from sewage sludge. **Journal of Analytical and Applied Pyrolysis**, v. 112, p. 284-289, 2015.

YUAN, P. et al. Review of biochar for the management of contaminated soil: preparation, application and prospect. **Science of the Total Environment**, v. 659, p. 473-490, 2018.

ZHANG, C. et al. Efficacy of carbonaceous nanocomposites for sorbing ionizable antibiotic sulfamethazine from aqueous solution. **Water Research**, v. 95, p. 103-112, 2016.

ZHANG, J. Effects of pyrolysis temperature and heating time on biochar obtained from the pyrolysis of straw and lignosulfonate. **Bioresource Technology**, v. 176, p. 288-291, 2015.

ZHANG, Q. et al. Temperature varied biochar as a reinforcing filler for high-density polyethylene composites. **Composites Part B: Engineering**, v. 175, p. 107151, 2019.

ZHAO, B. et al. Effect of pyrolysis temperature, heating rate, and residence time on rapeseed stem derived biochar. **Journal of Cleaner Production**, v. 174, p. 977-987, 2018.

ZHAO, R. et al. Effects of aged and fresh biochars on soil acidity under different incubation conditions. **Soil and Tillage Research**, v. 146, p. 133-138, 2015.

ZHOU, L. et al. Investigation of the adsorption-reduction mechanisms of hexavalent chromium by ramie biochars of different pyrolytic temperatures. **Bioresource Technology**, v. 218, p. 351-359, 2016

CHAPTER II - EFFECT OF PYROLYSIS TEMPERATURE ON EUCALYPTUS WOOD-DERIVED BIOCHAR ON AVAILABILITY AND TRANSPORT OF HEXAZINONE IN SOIL

ABSTRACT

Biochar is a material with adsorptive capacity that is able to prevent pollutant molecules reaching the local non-target. However, the ability to adsorb pollutants depends of pyrolysis temperature. In this research the effect of pyrolysis temperature (650, 750, 850 and 950 °C) on the properties of biochar derived from eucalyptus wood and its influence on the sorption/desorption, leaching and distribution of hexazinone in soil was evaluated. The properties hydrogen potential (pH), electrical conductivity (EC), ash content, yield, volatile matters (VM), elemental analysis (CHN-O), Fourier transform infrared spectroscopy (FT-IR), specific surface area (SSA) and volume of micropores (VM), and X-ray diffraction (XRD) were determined for all biochars produced. Sorption/desorption were investigated using the batch balance method and experiments were conducted to assess hexazinone leaching (in glass columns) and distribution (in biometric flasks). Increase in pyrolysis temperature to 950 °C increases (N + O)/C and ash ratios and produces a biochar with greater sorption (Kfs = 270.2 $\mu g^{(1 - 1/n)}$ $mL^{1/n}$ g^{-1}) and less desorption (Kfd = 222.3 $\mu g^{(1 - 1/n)}$ $mL^{1/n}$ g^{-1}) of hexazinone. The lower pyrolysis temperature of 650 °C produces an aliphatic material, with less sorption (Kfs = 50.4 $\mu g^{(1 - 1/n)}$ $mL^{1/n}$ g^{-1}) and greater desorption (Kfd = 39.6 $\mu g^{(1 - 1/n)}$ $mL^{1/n}$ g^{-1}). Biochars produced at pyrolysis temperatures of 850 and 950 °C completely prevented leaching of the herbicide in soil. The total hexazinone unavailable (mineralized + non-extractable residue) in biochar system produced at pyrolysis temperatures of 850 °C (46%) and 950 °C (49%) was higher compared to those produced at 650 °C (33%) and 750 °C (42%). Despite this, addition of biochar did not alter hexazinone mineralization, but reduced availability of the product in the environment due to the greater amount of non-extracted residue, thus reducing the risk of environmental contamination by this herbicide.

Keywords: Herbicide, immobilization, mineralization, retention, transport in soil profile.

1 INTRODUCTION

Chemical weed control is widely used in agriculture due to its high efficiency and low cost compared to other control methods. However, incorrect use of herbicides can cause damage to the environment and human health (HAN et al., 2019). Among negative effects caused by the application of herbicides, contamination of water sources due to leaching and runoff has often been reported in environmental monitoring studies (FENOLL et al., 2012; MACHADO et al., 2017; MASIOL et al., 2018; PORTAL et al., 2019). Herbicides with high solubility and low degradation have higher potential for water resources contamination.

Hexazinone, [3-cyclohexyl-6-(dimethylamino)-1-methyl-1,3,5-triazine-2- 4(1*H*,3*H*) dione] is an herbicide belonging to the triazinone group and is used in Brazil for pre- and post-emergence applications in sugarcane cultivation. (SHANER et al., 2014). This herbicide has high soil mobility and significant potential for contamination due to its high-water solubility of 33000 mg L^{-1} at 25 °C (KIM et al., 2018) and low sorption in soils (Kfs = 0.2 mg^{1-n} L^{n} kg^{-1}) (PEREIRA-JUNIOR et al., 2015). The characteristics of Brazilian soils combined with the properties of hexazinone mean that this herbicide is considered to possess high potential for environmental contamination (SILVA et al., 2019).

Strategies that reduce the transport capacity and availability of herbicides applied to soils can contribute to minimize environmental impacts. Among these strategies, the use of biochar is known to be a material with adsorptive capacity that is able to prevent pollutant molecules reaching the local non-target. However, the ability to adsorb pollutants depends on several factors, including those related to biochar production, such as pyrolysis temperature (SULIMAN et al., 2016), which can modify biochar properties, consequently changing its sorting capacity.

Biochar's efficiency in reducing herbicide mobility in soil is directly correlated with its sorption capacity (JONES et al., 2011; AZCARATE et al., 2015). High sorption of the herbicide to the biochar reduces the leaching potential of the product and prevents it from reaching the groundwater. However, in studies of the use of biochar for environmental decontamination it is also essential to assess the impact of the application of the carbonaceous sorbent on the persistence of herbicides. Applying biochar to soil can also decrease herbicide biodegradation due to high sorption and low desorption, resulting in lower availability for soil microorganisms (NAG et al., 2011; MUTER et al., 2014; KHORRAM et al., 2016). However, studies have shown that biochar can stimulate the soil microbiota, accelerating herbicide degradation (QIU et al., 2009; YVARI et al., 2019).

The use of plant materials for biochar production with potential herbicide environmental decontamination potential should take into account previous studies on the sorption and desorption capacity of material and the effects on herbicide behavior in biochar-modified soil. Changes in pyrolysis temperature can produce materials that are more or less efficient in reducing the potential for herbicide contamination. Therefore, the objectives of this research were: 1) to determine biochar's ability to reduce the availability of hexazinone; 2) to evaluate the effects of soil biochar application on hexazinone transport through leaching.

2 MATERIAL AND METHODS

2.1 Biochar production

Wood residues from the eucalyptus clone resulting from crossing *Eucalyptus urophylla* x *E. grandi* were ground into small pieces using a knife mill (Willey TE 340, Tecnal, São Paulo, Piracicaba, Brasil). Then powdery residues were sieved (2 mm) and dried in an oven with air circulation at 103 ±2 °C. Pyrolysis of the biomass was performed in a metal cylinder inside a muffle furnace (Q318M, Quimis, Diadema, São Paulo, Brasil). Carbonization was achieved at final temperatures of 650 (BC650), 750 (BC750), 850 (BC850) and 950 °C (BC950). The amount of residue used for each repetition was 200 ±10 g, temperature was increased at 1.7 °C min^{-1}, and after reaching final temperature it was kept for 1 h under limited air supply. After cooling, the biochar samples were ground, sieved (20 Mesh, <0.9 mm) and stored in a desiccator. In all experiments 1% (12 t ha^{-1}) of biochar was used in relation to the amount of soil added, allowing for a soil density of 1.200 kg m^{-3} and a soil tillage depth of 10 cm.

2.2 Soil collection and characterization

The soil sample, classified as Acrisol (WRB, 2006), was collected in Piracicaba-SP (22° 42’ 10” S; 47° 37’ 20” W), an agricultural area with no history of herbicide treatment. The sample was collected from the superficial layer (0–10 cm deep) after previous clearing of the vegetal layer. After collection, the sample was air dried for three days then sieved in a 2.0 mm sieve and stored at room temperature in an identified plastic bag. The soil sample was classified and analyzed for physical and chemical properties (Table 1).

Table 1. Physicochemical characteristics of the soil used in experiments.

pH_{CaCl2}	OC	P_{resina}	K	Ca	Mg	H+Al	SB	CEC	V
	g dm^{-3}	mg dm^{-3}	----------cmolc dm^{-3}----------						%
4.8	6.9	22	0.27	1.9	0.8	1.1	2.97	4.0	73
		Sand	**Silt**		**Clay**			**Texture class**	
----------g kg^{-1}----------									
		240	360		300			Medium Sandy	

Hydrogen potential (pH), organic carbon (OC); phosphorus (P); potassium (K); calcium (Ca); magnesium (Mg); potential acidity in SMP buffer (H+Al); sum of bases (SB); cation exchange capacity (CEC); base CEC saturation (V).

The methods used for chemical analysis were: pH in $CaCl_2$ 0.01 mol L^{-1}; phosphorus: by colorimetric method extracted with ion exchange resin; potassium: ion exchange resin extraction and determination in an atomic emission spectrophotometer; calcium and magnesium: ion exchange resin extraction and determination by atomic absorption spectrophotometer; potential acidity (H + Al): extracted with SMP buffer according to manual for chemical analysis and fertility assessment of tropical soils (RAIJ et al, 2001). To analyze the amount of sand, silt and clay, the Bouyoucos method was used (BOUYOUCOS, 1962).

2.3 Biochar characterization

To determine the amount of carbon (C), oxygen (O), hydrogen (H) and nitrogen (N), an elemental analyzer was used (Vario Macro Cube, Elementar, Cheadle Hulme, Reino Unido). Each 100 mg dried sample of biochar was weighed in a tin capsule, thereafter the capsule was closed and placed in the apparatus, which operates by subjecting the samples to combustion in an atmosphere of pure oxygen (99.999%). Gases formed by this combustion are measured using a thermal conductivity detector. Oxygen content was estimated by mass balance: O = 100 - (C + H + N + mineral).

The American Society for Testing and Materials (ASTM) method was used to determine the ash content (ASTM, 2018a) and volatile matters (MV) (ASTM, 2018b) of the biochar. To ensure reproducibility of measurements, each sample was analyzed in triplicate. Measurement of pH was performed according to ISO (2005). Electrical conductivity (EC) was determined using the BGK method (FCQAO, 1994).

The spatial arrangements of the samples and the presence of minerals were identified using the X-ray diffraction (XRD) technique in 0.5–5° and 10–80° 2θ bands, at low and medium angle using an XRD 6000 (Shimadzu, Kyoto, Japan), with radiation source of CuKα. (λ = 0.15406 nm), a nickel filter operating at 30 kV and 30 mA at a speed of 0.5° min^{-1}.

Surface functional groups were analyzed by Fourier transform infrared spectroscopy (FT-IR) (IRPrestige-21, Shimadzu, Tokyo, Japão) with wavelength range of 400–4000 cm^{-1} (for 64 scans with 4 cm^{-1} resolution).

Textural properties of the biochar surface were characterized using the Brunauer Emmett-Teller method (BET), which measures the physical adsorption of N_2 at 77 K with the aid of a surface area analyzer (ASAP-2020, Micromeritics, Norcross, GA, EUA), with relative pressure range (P/P_0) from 0.01 to 0.99. From the N_2 volume obtained in the assay and using the BET equation the specific surface area (SSA) and microporepore volume (MV) were determined.

The physicochemical analysis of eucalyptus wood biochars produced at different pyrolysis temperatures is shown in Table 2 and Figure 1.

Table 2. Physicochemical properties of eucalyptus-derived biochars.

Temp °C	EC µS	pH	C	H	N	O	H/C	O/C	N/C	(O+N)/C	Lignin (C-H)	Cellulose (OH)	870 (C-H)	MV	SSA	VM	Ash
			%											cm^3g	$m^2\ g^{-1}$	%	
650	134.3	9.4	87.1	1.60	0.0	10.7	0.02	0.12	0.00	0.12	0.02	0.10	0.33	0.05	410.5	11.9	0.63
750	164.6	9.5	87.7	0.87	1.1	9.5	0.01	0.11	0.01	0.12	0.01	0.13	0.02	0.07	402.5	5.5	0.84
850	161.6	9.4	88.0	0.89	1.3	9.0	0.01	0.10	0.01	0.12	0.01	0.14	0.02	0.08	362.9	3.4	0.84
950	273.1	9.3	86.9	0.18	1.4	10.7	0.00	0.12	0.02	0.14	0.02	0.11	0.01	0.02	224.4	3.6	1.06

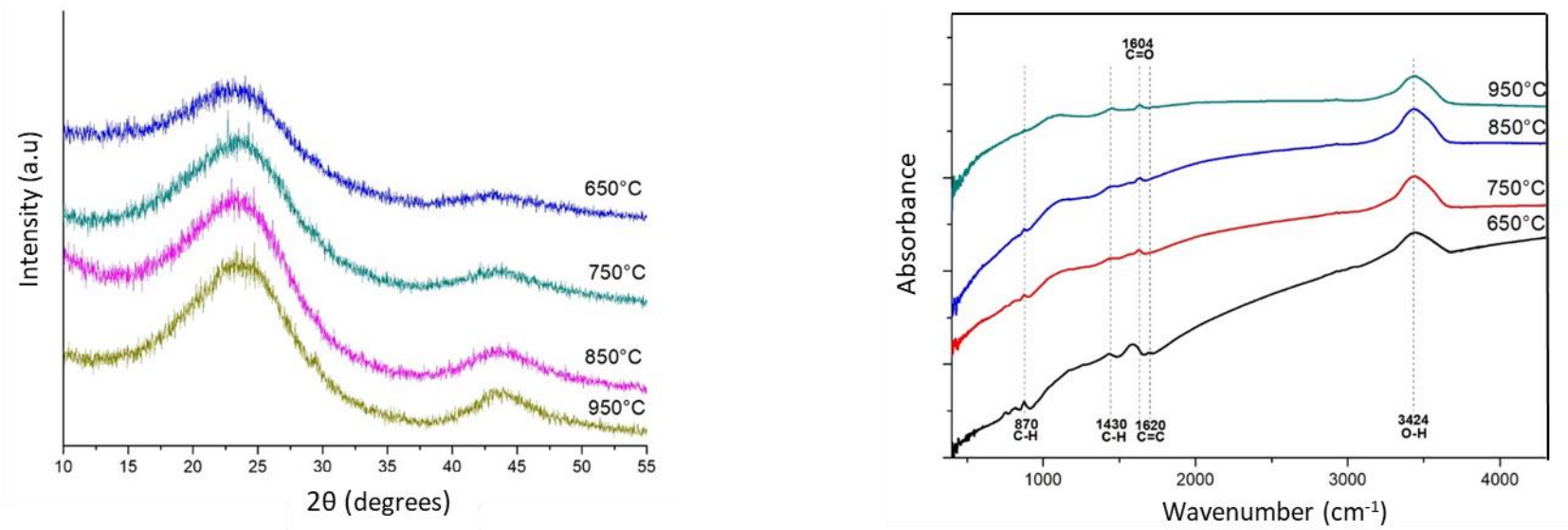

Figure 1. X-ray diffractometers (A) and FT-IR (B) spectra of eucalyptus-derived biochar samples produced at different pyrolysis temperatures.

2.4 Radiolabeled herbicide

Radiolabeled hexazinone [triazine-6-^{14}C] with specific activity of 3.14 MBq mg^{-1} and radiochemical purity of 99.7% (Izotop, Budapeste, Hungria) was used in the experiments. Doses were calculated based on the maximum recommended dose for sugarcane culture, 500 g a.i ha^{-1} (Nortox SA). To calculate the dose in each experiment, soil density was assumed to be 1.2 kg m^{-3} and the distribution of the herbicide in the first 10 cm of the soil profile was assumed to be homogeneous.

In the sorption experiment solutions were prepared with 0.013, 0.065, 0.13, 0.26 and 0.39 MBq L^{-1} of ^{14}C-hexazinone in $CaCl_2$ (0.01 mol L^{-1}), corresponding to concentrations of 4.17 (1%), 20.85 (5%), 41.7 (10%), 83.4 (20%) and 12.1 (30%) µg L^{-1} of active ingredient, respectively, in relation to the recommended dose.

For the leaching experiment the dose of radiolabeled herbicide was 66.85 MBq L^{-1} (21.29 mg L^{-1}), corresponding to 4.34% (21.7 g a.i. ha^{-1}) of the recommended dose, taking into account the area of the column where herbicide was applied was 19.625 x 10^{-6} m^2. In the distribution experiment, 11.66 kBq of radiolabeled herbicide per biometric flask was used, radioactivity that was recommended by the standard methodology (OECD, 2017), from a solution of 58.3 MBq L^{-1} (19.45 mg L^{-1}), corresponding to 13.7% (68.5 g a.i ha^{-1}) of the recommended dose. The solutions were prepared by dissolving ^{14}C-hexazinone standards in methanol.

2.5 Experimental design and treatments

All experiments were performed using a completely randomized design. For the sorption-desorption experiment biochar was used at four pyrolysis temperatures and five concentrations of ^{14}C-hexazinone. The leaching study was performed in a subdivided parcel. Parcels were untreated and biochar-treated soil at four pyrolysis temperatures. Subparcels were the eight depths (0–5, 5–10, 10–15, 15–20, 20–25, 25–30 cm, leachate and biochar). The distribution experiment was performed with five treatments (untreated and biochar-treated soil at four pyrolysis temperatures) over 84 days of incubation.

2.6 Sorption-desorption experiment

Experiments were performed according to the OECD 106: Adsorption – Desorption Using a Batch Equilibrium Method guideline (OECD, 2000). For sorption, 10 mL aliquots of the solutions of each concentration of ^{14}C-hexazinone in $CaCl_2$ (0.01 mol L^{-1}) were transferred to 50 mL Teflon flasks (experimental units) containing 100 mg of biochar at each temperature

of pyrolysis. Subsequently, the flasks were shaken on an orbital shaker table (Tecnal, MA02, Piracicaba, São Paulo, Brasil) in a dark room (20 ±2 °C) for a period of 24 h at 200 rpm to achieve equilibration time (Souza et al, 2018). After, the tubes had been centrifuged (CF16RXII. Hitachi. Tokyo. Japan) at 3000 rpm for 10 min aliquots of 1 mL of supernatant from each tube were transferred in duplicate to vials containing 10 mL of scintillating solution and analyzed using a liquid scintillation spectrometer (LSC) with a reading time of 5 min per sample (Tri-Carb 2910 TR, PerkinElmer, Waltham, Massachusetts, EUA) for determination of the equilibrium of ^{14}C-hexaxizone concentration in the solution (Ce). The amount of sorbed herbicide was calculated using the difference between initial concentration and supernatant concentration after equilibration.

The desorption experiment was performed immediately after sorption. The remaining supernatant from sorption experiment was removed and replaced with a new 10 mL solution of $CaCl_2$ (0.01 mol L^{-1}) in Teflon tubes containing biochar and sorbed ^{14}C-hexazinone. Tubes were again shaken on a horizontal shaker at 200 rpm in a dark room (20 ±2 °C) for 24 h to reach equilibrium concentration. Subsequently, tubes were centrifuged and 1 mL aliquots of the supernatant were pipetted in duplicate into scintillation vials containing 10 mL of scintillation solution and then analyzed by LSC. The amount desorbed was calculated as the difference between sorbed radioactivity in the soil and the remnant in the supernatant.

2.7 Leaching experiment

The methodology used for the leaching experiment followed OECD 312: Leaching in Soil Columns guidelines (OECD, 2002) with radiolabeled herbicides. Glass columns (50 cm length and 5 cm diameter) were prepared by placing glass wool on the conical tip of a funnel, followed by the addition of washed sand and the soil. Columns were filled to a depth of 30 cm. On top was 1% biochar from each pyrolysis temperature, the surface area of the column was assumed to be 19.625 x 10^{-6} m^2.

The glass columns filled with ~900 g of air-dried soil were placed in 1 L beakers containing a solution of 0.01 mol L^{-1} of calcium chloride ($CaCl_2$) to saturate the soil by capillary action. Afterwards, the columns were removed from the beakers and placed in supports until no further dripping was observed, in order to remove excess 0.01 M $CaCl_2$ solution. A 200 µL herbicide solution was pipetted evenly across the soil surface of the columns. Glass wool and an inverted glass funnel were placed on the soil surface to ensure that water distribution was adequate at the time of rain simulation.

Rain simulation using 0.01 mol L^{-1} $CaCl_2$ solution was performed using a peristaltic pump, previously calibrated to operate at a constant flow rate of 8.4 mL h^{-1} for 48 hours, totaling 200 mm of simulated rain. 1 L Schott flasks were placed at the base of the columns to collect total leachate, whose final volume was measured. A 10 mL volume of the leachate was transferred to 25 mL scintillation vials containing 10 mL Insta-gel plus (PerkinElmer, Waltham, Massachusetts, USA), then radioactivity was analyzed by the LSC for 15 min per sample.

Columns were removed from the support and placed in a horizontal position, interrupting flow. Afterwards, soil samples were taken from layers (at 0–5, 5–10, 10–15, 15–20, 20–25 and 25–30 cm) by injecting air into the tip of the column to force soil out. The layers were dried at room temperature, ground and homogenized in a mechanized mortar and pestle mill (Marconi, M001, Piracicaba, São Paulo, Brazil). Three 0.2 g subsamples were oxidized in a biological oxidizer for 3 min (RJ Harvey Instrument Corporation, Tappan, NY, USA). The high temperature causes ^{14}C to be released from the sample as ^{14}C-CO_2 and it is then captured in a 25 mL vial with 10 mL of scintillation solution and taken to the LSC for 5 min to quantify radioactivity. Results were expressed as a percentage of the total ^{14}C recovered. The balance of recovered radioactivity was calculated by summing ^{14}C of herbicide present in leachate, $^{14}CO_2$ recovered by oxidation of soil samples in each layer and biochars.

2.8 Hexazinone distribution experiment

In the hexazinone soil distribution experiment, the methodology used was based on the OEC guideline Aerobic and Anaerobic Transformation in Soil (OECD, 2017). Each experimental unit consisted of a biometric flask (Bartha; Pramer, 1965). The amount of dry soil recommended in the 50 g methodology was weighed into a 250 mL Bartha flask and 1% (m m^{-1}) was added. Water content was adjusted to 75% of field capacity and mixed with a glass rod. The control treatment consisted of herbicide soil without the addition of biochar. All experimental units were incubated in a dark room at 20 ±2 ºC for seven days to restore microbial metabolism equilibrium.

200 µL of ^{14}C hexazinone solution in 0.01 mol L^{-1} $CaCl_2$ were homogeneously applied with an automatic pipette. The contents of this solution were homogenized with a glass rod and vials were closed with a rubber cap coupled with a soda lime filter that absorbs CO_2, preventing its entry into the system. A 10 mL solution of 0.2 mol L^{-1} NaOH was placed in the side tube of the flasks to capture $^{14}CO_2$ from ^{14}C-hexazinone mineralization and also closed. The biometric flasks were incubated in a dark room at 20 ±2 ºC, according to the methodology for temperate

climates, for 84 days.

The 0.2 mol L^{-1} NaOH solution was changed weekly in all vials to avoid solution saturation. First, air was injected three times with aid of a 10 mL syringe to remove all the $^{14}CO_2$ that was not dissolved in the solution, then 1 mL of the NaOH solution was transferred to vials containing 10 mL of scintillation solution in order to read LSC radioactivity for 5 min per vial. Then a new 0.2 mol L^{-1} NaOH solution was added to capture the $^{14}CO_2$ which would be released. Mineralization was evaluated at 7, 14, 21, 28, 35, 42, 49, 56, 63, 70, 77 and 84 days after radiolabeled herbicide application. Finally, the total accumulated mineralized quantity was calculated and result expressed as a percentage of the total ^{14}C recovered.

Extraction of non-mineralized herbicide residue that remained in the soil + biochar treatments was performed at 0, 7, 28, 42, 56, 70 and 84 days after application of the product. Soil + biochar was transferred to a centrifuge in specific 500 mL propylene bottles. Then 100 mL of methanol was added to the soil samples and the tubes shaken for 1 h (200 rpm) on a Tecnal orbital shaker table (Model-MA02). Subsequently, tubes were centrifuged for 15 min at 3000 rpm and all supernatant was collected. This procedure was repeated twice more, but in the second and third extraction stages 80 and 70 mL of methanol were added, respectively (Guimarães et al., 2018). Two 1 mL aliquots of each extract were collected in vials containing 10 mL of scintillating solution and radioactivity was measured in the LSC for 5 min per vial. The amount of herbicide extracted from soil + biochar was represented by the sum of radioactivity from each extraction and the result expressed as a percentage of the total ^{14}C recovered.

After the extractions, the soils were oven dried at 40 °C for 24 h, weighed and homogenized in a soil mill. Three subsamples of 0.2 g were weighed and oxidized in a biological oxidizer and radioactivity readings were taken from LSC at 5 min per flask. The amount of radioactivity extracted from the treatment was determined by averaging the three samples taken from the three subsamples of total soil dry mass value and expressed as a percentage of total ^{14}C recovered, thus obtaining the amount of untreated waste.

2.9 Mass balance

In the leaching experiment, the recovered radioactivity balance was verified by summing percentages obtained as total leached plus the amount retained in the soil per experimental unit (OECD, 2002). For the soil distribution of hexazinone the radioactivity balance recovered was verified by summing percentages obtained by the release of $^{14}CO_2$ due

to mineralization, extraction of soil herbicides with methanol and oxidation of soil samples (OECD, 2017).

2.10 Statistical analysis

Correlations between pyrolysis temperatures and biochar properties were studied using Pearson's correlation analysis. Principal component analysis (PCA) was performed for the properties that were significant in the Pearson correlation and the results obtained in the sorption-desorption, leaching and distribution studies to determine the influence of these properties on the results.

Statistical analyses were performed using RStudio (v. 3.6.1) (R Core Team 2019). Sorption (Kfs) and desorption (Kfd) coefficients were compared by confidence interval ($p \leq 0.05$) obtained by isotherm regression analysis. Sorption-desorption coefficients were calculated using the Freundlich equation:

$$C_s = K_f \times C_e^{1/n}$$

where Cs is the concentration ($\mu g\ g^{-1}$) of sorbed hexazinone (after sorption or desorption) in biochar after equilibration; K*f* is the Freundlich equilibrium constant ($\mu g^{(1 - 1/n)}\ mL^{1/n}\ g^{-1}$); Ce is the concentration of hexazinone ($\mu g\ mL^{-1}$) after equilibrium; and 1/n is the degree of linearity of the isotherm. The hysteresis coefficient (H) for sorption-desorption isotherms was calculated using the following formula:

$$H = q_{desor} - q_{sorb} / q_{sorb}\ T, C$$

where; Qdesor is the solid phase concentration in the desorption and Qsorb is the amount in the solid phase in sorption at the same temperature (T) and the same concentration (C). Concentrations of 0.02, 0.04 and 0.06 $\mu g\ g^{-1}$ were used (HUANG et al., 1998; BHANDARI et al., 2001; RAN et al., 2004).

ANOVA was performed to examine the effects of biochars on soil ^{14}C-hexazinone leaching. Data for ^{14}C-hexazinone obtained in the soil layers did not show normal distribution of the residuals, therefore they were compared by confidence interval ($p \leq 0.05$). Averages for the mineralization ($^{14}C\text{-}CO_2$), extracted and non-extracted variables in untreated and biochar-treated soil produced at different pyrolysis temperatures were compared by confidence interval ($p \leq 0.05$) at 84 days of incubation.

3 RESULTS AND DISCUSSION

3.1 Principal component analysis (PCA) of the physicochemical properties of eucalyptus-derived biochars

PCA was performed among properties (O + N)/C, O/C, N/C, H/C, ash, cellulose (OH), MV and SSA, chosen based on Pearson's correction analysis (Appendix I) and the ability of the variable to explain sorption and desorption processes. For example, the properties C (%), N (%) and O (%) were excluded due to their high correlation (> 0.8) with other variables that demonstrated greater ability to characterize biochars ([O + N]/C, O/C, N/C, H/C) and, consequently, sorption and desorption in each material. Excluding some highly-correlated variables reduces multicollinearity problems in a PCA, allowing the analysis to consider only properties that best represent the variance between biochars. (DAS CHAGAS et al., 2019).

The results of the PCA of the selected properties produced three dimensions containing 100% of the cumulative variance (Figure 2). Dimensions 1 and 2 represented 96.9% of cumulative variance between biochars (Figure 2). The small contribution of Dimension 3 (3.1%) allowed the analysis to use only two dimensions, simplifying the interpretation of differences between biochars.

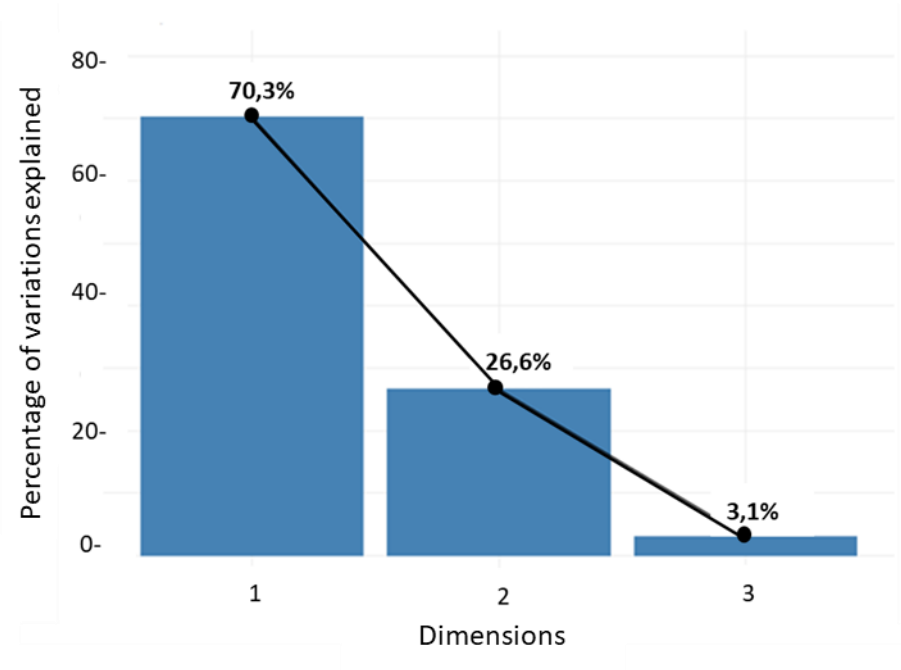

Figure 2. Dimensions and cumulative variance of principal component analysis of the physicochemical properties of eucalyptus-derived biochars.

Properties (O + N)/C (15.8), ashes (15.1) and SSA (14.2) contributed the largest variance in Dimension 1, compared to the other physicochemical properties (Figure 3). For Dimension 2, cellulose (OH), O/C and H/C showed greater contribution than the other attributes (Figure 3). Properties with the greatest contribution to variance considering Dimensions 1 and 2 were, in descending order, (O + N)/C > ashes > N/C > cellulose (OH) > H/C > SSA≈ MV (Figure 3).

Pyrolysis temperature altered the physicochemical properties of eucalyptus-derived biochars. However, some properties changed more due to the increase in pyrolysis temperature, and consequently allowed us to differentiate between biochars. BC950 was located in the direction of the vectors of the variables (O + N)/C and ashes indicating a positive correlation and higher absolute values for these properties in comparison to BC650, BC750 and BC850 (Figure 3).

The positive correlation between high pyrolysis temperature and higher ash content is related to the minerals that remain in biochar after the loss of more volatile compounds at high temperatures (YUAN et al., 2015; WEBER; QUICKER, 2018). Generally, the (O + N)/C ratio is lower when higher pyrolysis temperatures are used to synthesize biochars (SULIMAN et al., 2016; LEE et al., 2017; ZHAO et al., 2018). However, complex structures containing oxygen and nitrogen in raw materials can limit the loss of these atoms after the pyrolysis process.

Eucalyptus has a high amount of lignin that can inhibit the release of oxygen in byproducts (bio-oil or biogas) at high pyrolysis temperatures (HEIDARI et al., 2014). No correlation between N content and pyrolysis temperature has been reported in the literature. However, the increase noted in BC950 nitrogen content could occur due to the decrease of other components during the volatilization process. (WEBER; QUICKER, 2018).

The cellulose (OH) and MV vectors were positioned in the same quadrant as BC750 and BC850, demonstrating that these biochars show greater physicochemical similarity (Figure 3). SSA and H/C differentiated BC650 from other biochars (Figure 3).

BC650, BC750 and BC850 have more aliphatic properties, with higher SSA and VTP compared to BC950. BC650 showed a higher number of aliphatic structures compared to BC750 and BC850. Loss of aliphatic groups occurs when materials are elevated to high pyrolysis temperatures due to the release of gases (CH_4 and H_2) (Weber; Quicker, 2018). The number of hydroxyl groups (O-H) increased when the pyrolysis temperature increased from 650 to 850 °C, and this was the main difference detected between BC650, BC750 and BC850.

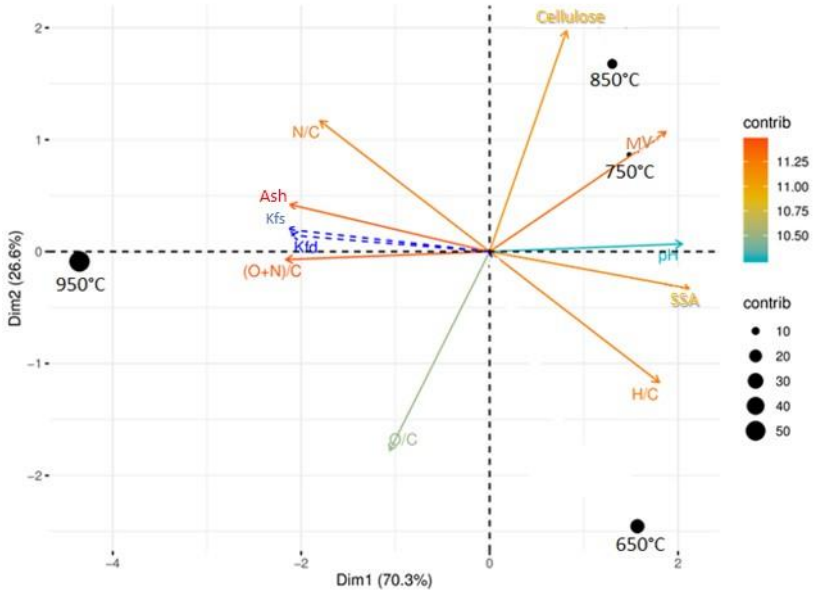

Figure 3. Principal component analysis (PCA) of the physicochemical properties of eucalyptus-derived biochars produced at different pyrolysis temperatures.

3.2 Hexazinone sorption-desorption in biochars produced at different pyrolysis temperatures

The Freundlich models for hexazinone sorption and desorption in eucalyptus-derived biochars demonstrated good adjustments for all pyrolysis temperatures, with R^2 values ranging from 0.93 to 0.99 (Table 4) and values of $1/n_{sorption}$ and $1/n_{desorption}$ less than 1.0 for all biochars (Table 4). In descending order, the values of $1/n_{sorption}$ were BC950 (0.90) > BC650 (0.85) > BC850 (0.64) > BC750 (0.62) (Table 4). For desorption, values in descending order for $1/n_{desorption}$ were similar to those of sorption among biochars, BC950 (0.95) > BC650 (0.90) > BC850 (0.74) > BC750 (0.59) (Table 4).

Values of $1/n_{sorption}$ smaller than one unit (1.0) indicate L-type isotherms (Figure 4). This type of isotherm is characteristic of sorbates with lower sorption capacity at high sorbate concentrations (ALCHOUR et al., 2019). At low concentration hexazinone molecules are rapidly sorbed to biochars due to the high availability of regions capable of sorb this herbicide. However, after sorption of hexazinone molecules, the number of binding sites becomes limited and competition between the molecules present in solution increases, reducing the sorption rate of biochars. (MENDES et al, 2019; DOS SANTOS et al., 2019).

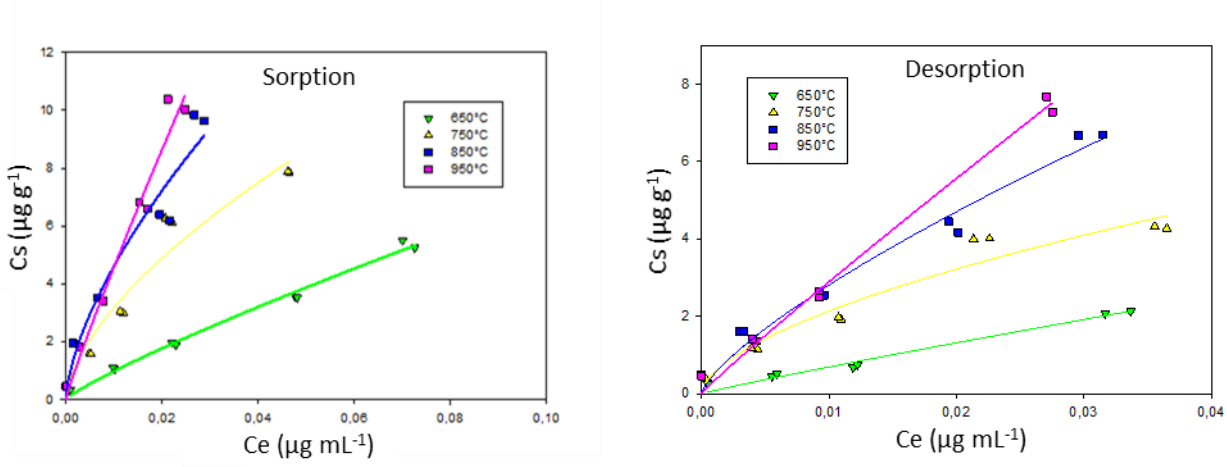

Figure 4. Relationship between amount of sorbed ^{14}C-hexazinone (Cs) and solution (Ce) and Freundlich sorption (a) and desorption (b) isotherms in biochars derived from eucalyptus wood produced at different pyrolysis temperatures.

Increasing pyrolysis temperature for biochar production increased the Kfs value (Table 3). The lowest Kfs value for hexazinone was observed in BC650 (50.4 $\mu g^{(1 - 1/n)}$ $mL^{1/n}$ g^{-1}). Kfs values for BC750 and BC850 were 55.1 and 90.1 $\mu g^{(1 - 1/n)}$ $mL^{1/n}$ g^{-1}, respectively. The highest Kfs value was observed for BC950 (270.2 $\mu g^{(1 - 1/n)}$ $mL^{1/n}$ g^{-1}).

Table 3. Freundlich isotherm parameters for sorption (Kfs, $1/n_{sorption}$) and desorption (Kfd, $1/n_{dessorção}$) and sorbed and desorbed percentage of hexazinone in eucalyptus-derived biochars produced at different pyrolysis temperatures.

Sorption	Temperature (°C)	Kfs $\mu g^{(1 - 1/n)}$ $mL^{1/n}$ g^{-1}	R^2	$1/n_{sorption}$	% sorbed
	650	50.4 (±1.10)	0.99	0.85 (±0,02)	52
	750	55.1 (±2.04)	0.94	0.62 (±0.02)	58
	850	90.1 (±10.12)	0.95	0.64 (±0.02)	76
	950	270.2 (±14.18)	0.93	0.90 (±0.01)	85
Desorption	Temperature (°C)	Kfd $\mu g^{(1 - 1/n)}$ $mL^{1/n}$ g^{-1}	R^2	$1/n_{desorption}$	% desorbed
	650	39.6 (±3.10)	0.96	0.90 (±0.04)	30
	750	49.5 (±5.2)	0.95	0.59 (±0.04)	27
	850	86.0 (±5.20)	0.97	0.74 (±0.02)	21
	950	222.3 (±11.92)	0.98	0.94 (±0.03)	14
Hysteresis	Temperature (°C)	Cw 0.02 µg mL^{-1}	Cw 0.04 µg mL^{-1}	Cw 0.06 µg mL^{-1}	
	650	-0.33	-0.30	-0.27	
	750	-0.19	-0.21	-0.22	
	850	-0.35	-0.31	-0.28	
	950	-0.30	-0.28	-0.26	

Values correspond to means and lower (-) and upper (+) confidence intervals (CI) ($p \leq 0.05$).

BC650 showed the lowest sorption capacity for hexazinone. This biochar was the most aliphatic compared to the others, indicating that a greater number of C-H groups in biochars will provide lower hexazinone sorbent capacity. The solubility of hexazinone in hexane is extremely low (3 mg L^{-1}), explaining the poor affinity for more aliphatic compounds like BC650. In addition, the high solubility of hexazinone in water (33,000 mg L^{-1}) favors the existence of hexazinone molecules in aqueous phase, making BC650 sorption difficult.

The loss of aliphatic groups in BC750 and B850 produced higher hexazinone sorption capacity (58% and 76%, respectively) compared to BC650. The higher affinity of hexazinone to BC750 and BC850 enables surface bond formation due to intermolecular forces (Van der Waals) between the non-polar regions of biochars and hexazinone. Regarding BC850 and BC750, the higher sorption observed in BC850 is due to the higher number of hydroxyl groups (O-H) present in this biochar structure. An abundance of O-H groups in BC850 favors a greater number of hydrogen bonds with hexazinone. This herbicide has two regions capable of establishing hydrogen bonds (Table 2), increasing the number of molecules adsorbed on surfaces with a higher number of hydroxyls. Wang et al. (2019) identified the high capacity of triazines (including hexazinone) and their residues to establish hydrogen bonds via N-H groups with carboxyls present in sorbents.

The increase in pyrolysis temperature to 950 °C in the eucalyptus derivative increased the aromaticity of the biochar produced. Possibly such higher aromaticity favored hexazinone partitioning in the carbonaceous material due to the higher solubility of this herbicide in compounds with aromatic structures, such as chloroform (3880 g kg^{-1}), benzene (940 g kg^{-1}) and toluene (386 g kg^{-1}), when compared to aliphatic structures. In addition, hexazinone has a polar surface (56.2 $Å^2$, see Table 2) that can be attracted to the polar regions of BC950. The higher ash concentration and (O + N)/C ratio noted in the structure of BC950 may lead to greater electron redistribution due to the electronegativity differences of the atoms (WEBER; QUICKER, 2018), increasing the polarity of the material attracting hexazinone.

Increased sorption capacity in BC950 could also be due to the occurrence of $\pi - \pi$-type bonds between hexazinone and BC950. The polyaromatic surfaces of biochars are rich in π-electrons that can interact with nitroaromatic (π-electron poor) groups present in triazines, forming $\pi - \pi$ electron acceptor/donor bonds. (XIAO; PIGNATELLO, 2015a). This kind of interaction has already been evidenced for ametryn and prometon (XIAO; PIGNATELLO, 2015b).

The lowest Kfd value for hexazinone was observed for BC650 (39.6), followed by BC750 (49.5), BC750 (86.0) and BC950 (222.3) (Table 3). Regardless of pyrolysis

temperature, eucalyptus-derived biochars showed negative H for the calculated concentrations (Cw) (Table 3). Higher pyrolysis temperature produced lower desorption biochars for hexazinone. Greater partition and attraction and the establishment of π – π bonds due to BC950's increased aromaticity, polarity and π-electrons increases the stability of the biochar-hexazinone interaction, making it difficult for the herbicide molecule to return to the soil solution. For BC750 and BC850, hydrogen bonds may possibly be responsible for the lower desorption of hexazinone, especially BC850 which showed lower desorption than BC750. BC650 allowed higher desorption of hexazinone compared to other biochars, indicating weak interaction between biochar and hexazinone.

Despite the lower desorption capacity observed in BC750, BC850 and BC950, all biochars showed negative H for hexazinone. Negative values for this index indicate a greater tendency for hexazinone to return to the soil water phase after successive desorption steps, where a metastable state between biochar and herbicide is not achieved.

3.3 Hexazinone leaching in soil treated with eucalyptus wood biochars produced at different temperatures

The mass balance for the leaching experiment was 109.3%, 91.8%, 88.3%, 81.7% and 106.1% for BC650, BC750, BC850 and BC950 biochars treatments and the control, respectively. These values were above the recommended minimum (80%) (NANDULA; VENCILL, 2015) and below the recommended maximum (110%) (OCDE, 2002).

Hexazinone percolated through the entire soil column (30 cm) after 200 mm of precipitation on the untreated soil (Figure 5E). In addition, hexazinone was quantified (2%) in the leachate in untreated soil. The largest amount of hexazinone detected in the columns was in the 10–15 cm (26%) and 15-20 cm (27%) layers of the untreated soil (Figure 5).

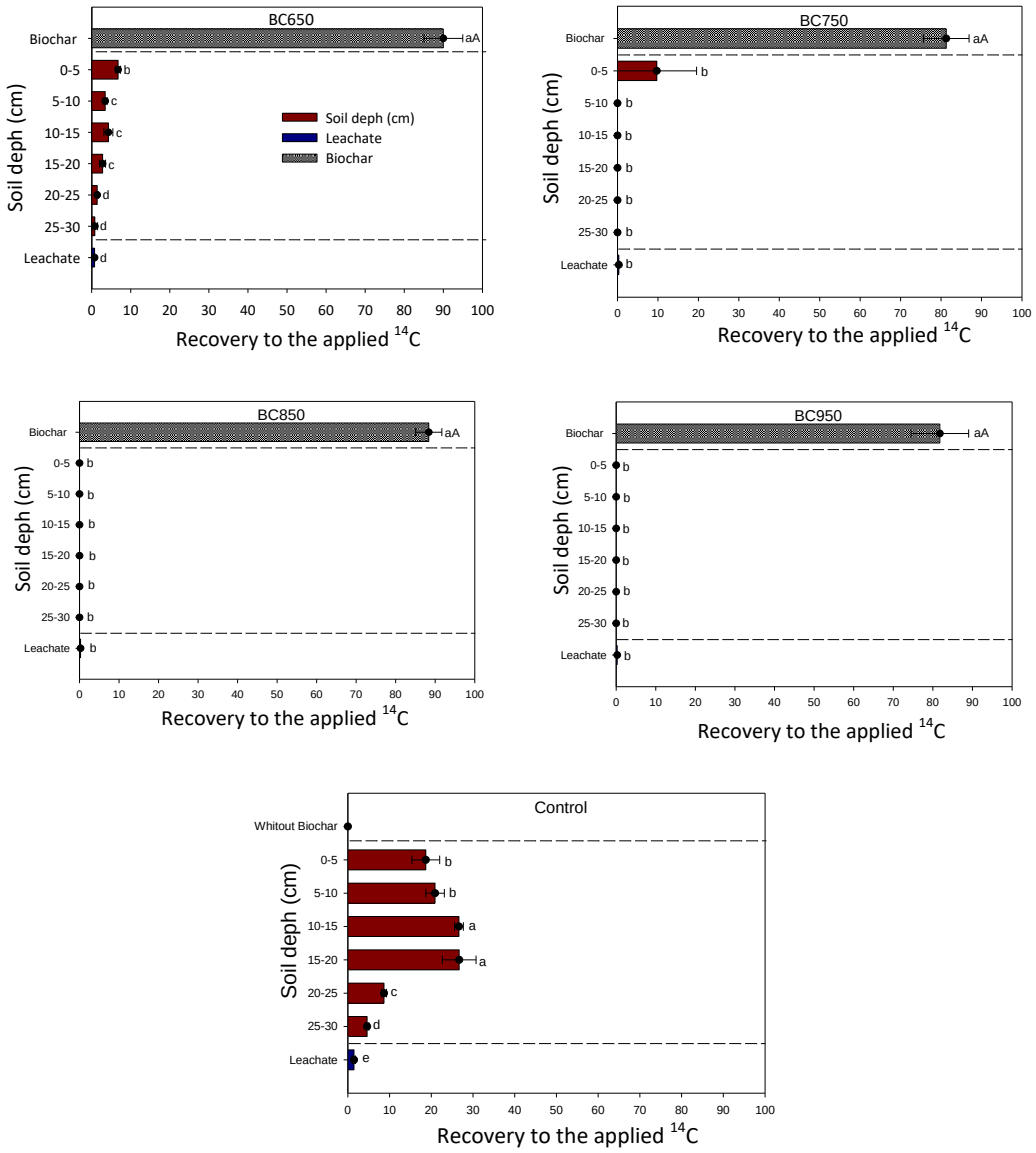

Figure 5. Percentage hexazinone distributed in columns after precipitation of 200 mm for 48 h in non-biochar treated soil (control) and biochar-treated soil (1%); eucalyptus wood processed at different pyrolysis temperatures. Bars represent the standard deviation of duplicates and lowercase letters represent a significant difference between layers using the confidence interval of the mean ($p \leq 0.05$, $n = 2$).

Hexazinone has shown high levels of leaching in the soil untreated with biochar. The high solubility of this herbicide allowed its molecules to percolate through all soil layers, with a small amount founded in leachate. Larger amount of the hexazinone was accumulated in the deeper layers (10–20 cm). Similar to that reported by other experiments (MENDES et al., 2016; DOS REIS et al., 2017), hexazinone showed high potential for contaminating groundwater. In addition to the contamination caused by the high degree of leaching, accumulation of hexazinone in deeper soil layers can extend the persistence of these molecules in the environment. The activity of aerobic microorganisms is lower in deep soil regions due to lower

oxygen concentration (CLARK et al., 2019), limiting the degradation of hexazinone by aerobic microbiota. Anaerobic condition can be extremely disadvantageous for the dissipation of hexazinone; degradation of this herbicide is not observed under these conditions (CALDERON et al., 2004; RHODES et al., 1980).

In soil treated with BC650, hexazinone was detected in all layers of the soil and it leached (Figure 5). The largest amount recovered in the soil column was observed in the 0–5 cm layer (8%). In the presence of BC750, hexazinone percolated only to the 0–5 cm layer (10% recovered). No hexazinone leaching was detected in BC850- and BC950-treated soil.

When higher temperature pyrolysis was used to synthesize biochar, this material retained hexazinone molecules in surface layers of the soil with greater efficiency. Although leaching of hexazinone was found throughout the column in the soil treated with BC650, biochar produced at higher temperatures reduced the amount of herbicide leached into all soil layers. BC750, BC850 and BC950, and especially the last two, demonstrated greater efficiency in preventing contamination of ground water compared to BC650 since hexazinone molecules were retained in surface soil layers. Lower mobility due to the application of hexazinone biochars results from the sorptive capacity of these materials for this herbicide. That is, the greatest retention of hexazinone is achieved when materials with higher sorption capacity are applied to the soil, such as BC850 and BC950. For a range of different herbicides, biochar's sorption capacity is positively correlated with its potential to reduce the mobility of molecules in soil (TAHIR et al., 2016; TRIGO et al., 2016; MENDES et al., 2018).

3.4 Hexazinone distribution in soil with eucalyptus wood biochars produced at different temperatures

For the distribution experiment, mass balances were 97.6%, 97.2%, 95.9%, 95.7% and 93.6% for biochar treatments BC650, BC750, BC850, BC950 and control, respectively. These values were between the minimum (90%) and maximum (110%) recommended (OECD, 2017).

^{14}C-CO_2 mineralization increased with incubation time, stabilizing at 56 days, followed by a reduction in all treatments (Figure 6). Soil not treated with biochar showed higher mineralization of ^{14}C-CO_2 (6.02%) compared to treated soils BC650 (4.75%), BC750 (4.65%), BC850 (4.54%) and BC950 (4.23%) (Figure 6).

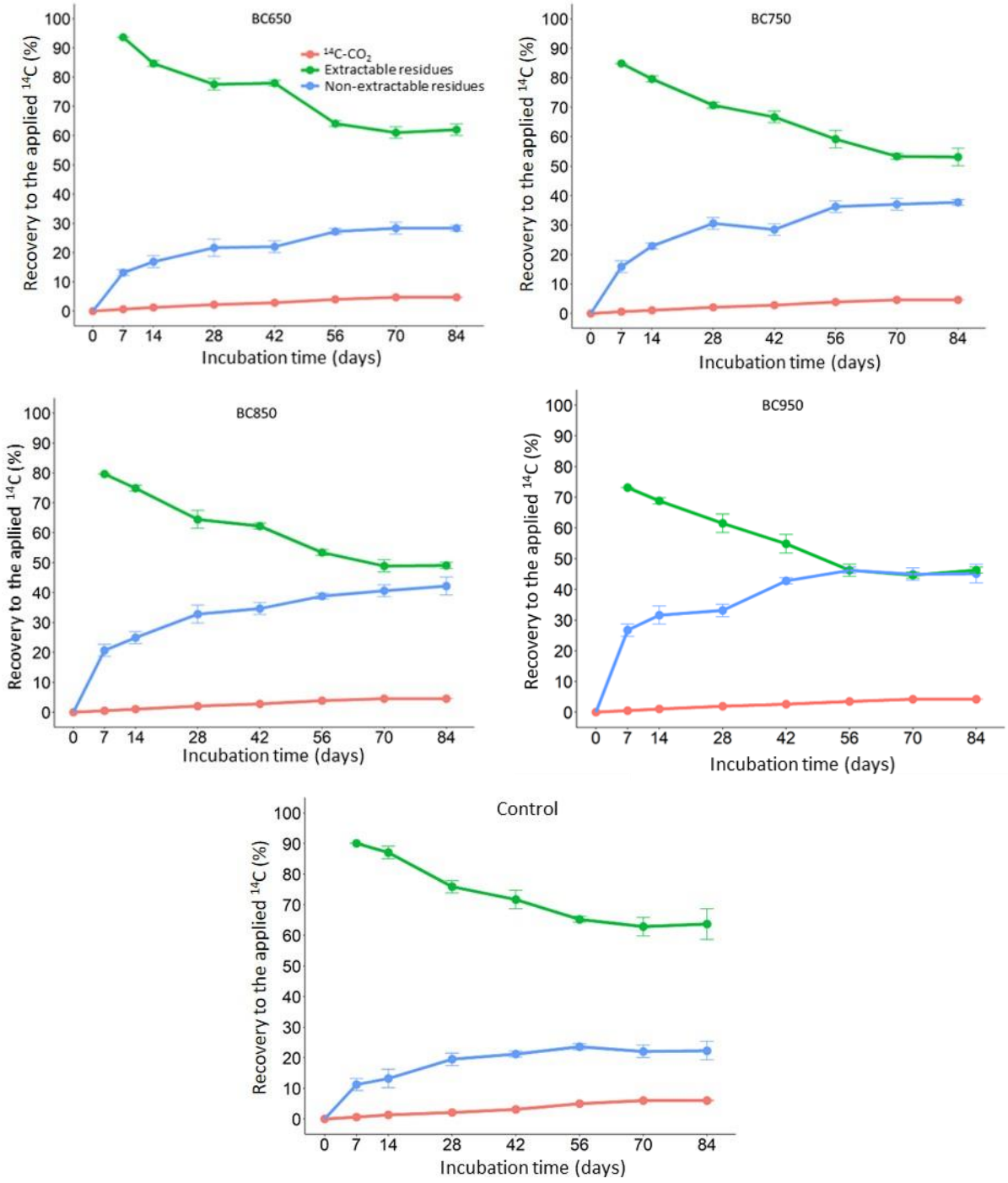

Figure 6. Percentage of ^{14}C (%) recovered in non-biochar (control) and biochar-treated (1%) soil during 84 days of incubation. Biochar produced at different pyrolysis temperatures. Vertical bars represent confidence interval of mean ($p \leq 0.05$, $n = 2$).

The low amount of ^{14}C-CO_2 recovered from untreated and biochar-treated soil does not necessarily imply that the hexazinone mineralization process was low. The major metabolites generated due to microbial degradation of hexazinone involve 5-triazine carbon demethylation, N-dealkylation of the dimethylamino group or substitution of the dimethylamino group by

oxygen (WANG et al., 2005; WANG et al., 2012), which causes an intense evolution of CO_2. However, carbon has been radiolabeled at the 6-triazine position of the hexazinone molecule and this structure exhibits greater stability and resistance to degradation by microorganisms (ERICKSON et al., 1989; KAUFMAN AND KEARNEY et al., 1970), consequently resulting in low release of ^{14}C-CO_2. Despite the low mineralization observed in the treatments, it can be inferred that hexazinone can be completely degraded to low environmental toxicity monomers. S-triazine ring breakdown involves specific bacteria (strains of *Frankia* sp.) that produce enzymes that can open the ring to use carbon and nitrogen as a source of nutrients (REHAN et al., 2017).

For residues not extracted at 84 days of incubation, the ^{14}C values recovered in the control BC650, BC750, BC850 and BC950 were 22%, 28%, 3%7, 42% and 45%, respectively (Figure 6). Total unavailable hexazinone (mineralized + non-extractable residue) in BC850 (46%) and BC950 (49%) was higher compared to BC650 (33%) and BC750 (42%) (Figure 6). Despite lower mineralization in BC850 and BC950, these biochars demonstrated the highest sorption capacity for hexazinone, allowing the herbicide to be immobilized in its structure as a non-extracted residue. However, it is important to note that part of the hexazinone immobilized as non-extracted can be strongly absorbed or trapped in biochar micropores (non-extractable residue type I); in this type of compartmentalization, as non-extracted residue, the herbicide is capable of returning to the environment (KAESTNER et al., 2014), and this behavior can prolong hexazinone persistence in BC850- and BC950-treated soils. Claben et al. (2019) observed that 25% of the radioactivity recovered as non-extracted residue was related to the main compound (dodecyl benzyl trimethylammonium chloride) and that this compound could return to the environment at slower rates.

Higher sorption of BC850 and BC950 can mean a reduced amount of available hexazinone, explaining lower mineralized percentage. There is no fixed correlation between percentage of herbicide sorbed as non-extracted residue and the mineralization process in biochar treated soils. For example, for Diuron, in soil treatments with both fresh and aged biochars, sorption increased and mineralization of the herbicide did not alter (ZHELEZOVA et al., 2017). Atrazine also showed similar behavior, with a similar mineralization rate between untreated and biochar-treated soil (JABLONOWSKI et al., 2013). However, other herbicides like Bentazone (MUKHERJEE et al., 2016), isoproturon (REID et al., 2013) and simazine (JONES et al., 2011) have already shown a significant reduction in amounts mineralized in biochar-treated soils due to the large amount compartmentalized as non-extractable residue.

BC850 and BC950 showed high sorption and low desorption for hexazinone. This reduced the availability of herbicide molecules in the soil water phase, preventing the herbicide leaching into soil. The mechanism that allowed the highest sorption in these biochars was different according to the inherent physicochemical properties of each one. BC650 and BC750 reduced the amount of hexazinone leached compared to untreated soil, but some of molecules were able to percolate through soil layers due to the lower sorption and greater desorption of herbicide in these materials. Sorption of hexazinone to biochars did not cause major changes in the molecule mineralization process, resulting in a minimal difference in the amount of $^{14}CO_2$ evolved between untreated and biochar-treated soil. In general, the addition of biochars established a sorption that resulted in higher formation of non-extractable residues, decreasing the amount of hexazinone available in the system, with more positive effects for biochars produced at temperatures above 850 °C.

Addition of BC650, BC750, BC850 and BC950 decreased hexazinone mobility and availability in soil, reducing the risk of environmental contamination by this herbicide. However, lower amounts of hexazinone available in the soil can reduce the effectiveness of weed control due to lower product concentration. In addition to lower availability, lower hexazinone leaching can impair control of the seed bank located deeper in the soil.

4 CONCLUSIONS

Pyrolysis temperature alters the properties of biochar produced from eucalyptus wood. Increasing pyrolysis temperature to 950 °C raises the (N + O)/C and ash ratios and provides a higher sorption and lower desorption capacity for hexazinone. A pyrolysis temperature of 650 °C produces a low-sorption, high-desorption aliphatic material for hexazinone. Eucalyptus-derived wood biochars produced at a pyrolysis temperature of 850 or 950 °C can prevent hexazinone leaching into soil. Addition of this biochar produced at all temperatures does not change the hexazinone mineralization process, but reduces the availability of the herbicide in the environment by trapping greater amounts as non-extractable residues. Biochars pyrolyzed at 850 and 950 °C are the most efficient at reducing potential hexazinone contamination in soils.

REFERENCE

AICHOUR, A. et al. Highly brilliant green removal from wastewater by mesoporous adsorbents: Kinetics, thermodynamics and equilibrium isotherm studies. **Microchemical Journal**, v. 146, p. 1255-1262, 2019.

ASTM. American Society for Testing and Materials. **Standard Test Method for Ash in the Analysis Sample of Coal and Coke from Coal.** D3174 – 12 (2018a). Disponível em: < https://compass.astm.org/EDIT/html_annot.cgi?D3174+12(2018)>. Acesso em: 12 de out de 2019.

ASTM. American Society for Testing and Materials. **Standard Test Method for Volatile Matter in the Analysis Sample of Coal and Coke.** D3175 (2018b). Disponível em: < https://compass.astm.org/EDIT/html_annot.cgi?D3175+18>. Acesso em: 12 de out de 2019.

AZCARATE, M. et al. Sorption, desorption and leaching potential of sulfonylurea herbicides in Argentinean soils. **Journal of Environmental Science and Health, Part B,** v. 50, n. 4, p. 229-237, 2015.

RAIJ, B. V. **Análise química para avaliação da fertilidade de solos tropicais**. IAC, 2001.

BGK **Methodenbuch zur Analyse von Kompost (BGK e.V.) [Methods Book for the Analysis of Compost, Federal Compost Quality Assurance Organisation (BGK e.V.)]**Abfall Now (Hrsg.), Stuttgart, 1994.

BHANDARI, A. et al. Impact of peroxidase addition on the sorption−desorption behavior of phenolic contaminants in surface soils. **Environmental Science & Technology**, v. 35, n. 15, p. 3163-3168, 2001.

BOUYOUCOS, G. Hydrometer method improved for making particle size analyses of soils. **Agronomy Journal**, v. 54, n. 5, p. 464-465, 1962.

CALDERON, M. J. et al. Hexazinone and simazine dissipation in forestry field nurseries. **Chemosphere**, v. 54, n. 1, p. 1-8, 2004.

CLARK, J. D. et al. United States midwest soil and weather conditions influence anaerobic potentially mineralizable nitrogen. **Soil Science Society of America Journal**, v. 83, n. 4, p. 1137-1147, 2019.

CLABEN, D. et al. Formation, classification and identification of non-extractable residues of ^{14}C-labelled ionic compounds in soil. **Chemosphere**, v. 232, p. 164-170, 2019.

DAS CHAGAS, P. S. F. et al. Multivariate analysis reveals significant diuron-related changes in the soil composition of different Brazilian regions. **Scientific Reports**, v. 9, n. 1, p. 7900, 2019.

DOS REIS, F. C. et al. Leaching of diuron, hexazinone, and sulfometuron-methyl applied alone and in mixture in soils with contrasting textures. **Journal of Agricultural and Food Chemistry**, v. 65, n. 13, p. 2645-2650, 2017.

DOS SANTOS, L. O. G. et al. Effect of liming on hexazinone sorption and desorption behavior in various soils. **Archives of Agronomy and Soil Science**, v. 65, n. 9, p. 1183-1195, 2019.

ERICKSON, L. et al. Degradation of atrazine and related S-triazines. **Critical Reviews in Environmental Science and Technology**, v. 19, n. 1, p. 1-14, 1989.

FENOLL, J. et al. Trace analysis of sulfonylurea herbicides in water samples by solid-phase extraction and liquid chromatography-tandem mass spectrometry. **Talanta,** v. 101, p. 273-282, 2012.

HAN, M. et al. Persistent organic pollutants, pesticides, and the risk of thyroid cancer: systematic review and meta-analysis. **European Journal of Cancer Prevention**, v. 28, n. 4, p. 344-349, 2019

HEIDARI, A. et al. Effect of process conditions on product yield and composition of fast pyrolysis of *Eucalyptus grandis* in fluidized bed reactor. **Journal of Industrial and Engineering Chemistry**, v. 20, n. 4, p. 2594-2602, 2014.

HUANG, W. et al. Hysteresis in the sorption and desorption of hydrophobic organic contaminants by soils and sediments: 1. A comparative analysis of experimental protocols. **Journal of Contaminant Hydrology**, v. 31, n. 1-2, p. 129-148, 1998.

ISO, International Standards Organization. **Soil Quality–Determination of pH (ISO 10390: 2005)**. Disponível em: < https://www.iso.org/standard/40879.html>. Acesso em: 12 de Out. de 2019.

JABLONOWSKI, N. et al. Biochar-mediated [^{14}C] atrazine mineralization in atrazine-adapted soils from Belgium and Brazil. **Journal of Agricultural and Food Chemistry**, v. 61, n. 3, p. 512-516, 2013.

JONES, D. L.et al. Biochar mediated alterations in herbicide breakdown and leaching in soil. **Soil Biology and Biochemistry**, v. 43, n. 4, p. 804-813, 2011.

KAESTNER, M. et al. Classification and modelling of nonextractable residue (NER) formation of xenobiotics in soil–a synthesis. **Critical Reviews in Environmental Science and Technology**, v. 44, n. 19, p. 2107-2171, 2014.

KAUFMAN, D. D.; KEARNEY, P. C. Microbial degradation of s-triazine herbicides. In: Single Pesticide Volume: **The Triazine Herbicides**. Springer, New York, NY, 1970. p. 235-265.

KHORRAM, M. S. et al. Dissipation of fomesafen in biochar-amended soil and its availability to corn (*Zea mays* L.) and earthworm (*Eisenia fetida*). **Journal of Soils and Sediments**, v. 16, n. 10, p. 2439-2448, 2016.

KIM, S. et al. PubChem 2019 update: improved access to chemical data. **Nucleic Acids Research**, v. 47, n. 1, p. 1102-1109, 2018.

LEE, X. J. et al. Biochar potential evaluation of palm oil wastes through slow pyrolysis: Thermochemical characterization and pyrolytic kinetic studies. **Bioresource Technology**, v. 236, p. 155-163, 2017.

MACHADO, C. S. et al. Health risks of environmental exposure to metals and herbicides in the Pardo River, Brazil. **Environmental Science and Pollution Research**, v. 24, n. 25, p. 20160-20172, 2017.

MASIOL, M. et al. Herbicides in river water across the northeastern Italy: occurrence and spatial patterns of glyphosate, aminomethylphosphonic acid, and glufosinate ammonium. **Environmental Science and Pollution Research**, v. 25, n. 24, p. 24368-24378, 2018.

MENDES, K. F. et al. Animal bonechar increases sorption and decreases leaching potential of aminocyclopyrachlor and mesotrione in a tropical soil. **Geoderma**, v. 316, p. 11-18, 2018.

MENDES, K. F. et al. Leaching of a mixture of hexazinone, sulfometuron-methyl, and diuron applied to soils of contrasting textures. **Water, Air, & Soil Pollution**, v. 227, n. 8, p. 268, 2016.

MUKHERJEE, S. et al. Dissipation of bentazone, pyrimethanil and boscalid in biochar and digestate based soil mixtures for biopurification systems. **Science of the Total Environment**, v. 544, p. 192-202, 2016.

MUTER, O. et al. Evaluation of the changes induced by gasification biochar in a peat-sand substrate. **International Agrophysics**, v. 28, n. 4, p. 471-478, 2014.

NAG, S. K. et al. Poor efficacy of herbicides in biochar-amended soils as affected by their chemistry and mode of action. **Chemosphere**, v. 84, n. 11, p. 1572-1577, 2011.

NANDULA, V. K.; VENCILL, W. K. Herbicide absorption and translocation in plants using radioisotopes. **Weed Science**, v. 63, n. SP1, p. 140-151, 2015.

OECD. Organisation for Economic Co-Operation and Development. **OECD Guidelines for Testing of Chemicals. Test Number 312: Leaching in Soil Columns OECD, Paris (2004).** Disponível em: <https://www.oecd-ilibrary.org/environment/test-no-312-leaching-in-soil-columns_9789264070561-en>. Acesso em: 5 de Out. de 2018

OECD. Organisation for Economic Co-Operation and Development. **OECD Guidelines for Testing of Chemicals. Test Number 307: Aerobic and Anaerobic Transformation in Soil OEDC, Paris (2002).** Disponível em: < https://www.oecd-ilibrary.org/environment/test-no-307-aerobic-and-anaerobic-transformation-in-soil_9789264070509-en>. Acesso em: 5 de Out. de 2018

OECD. Organisation for Economic Co-operation and Development. **OECD Guidelines for the Testing of Chemicals. Test Number 106, Adsorption – Desorption Using a Batch Equilibrium Method, OECD: Paris (2000).** Disponível em: <https://www.oecd-ilibrary.org/environment/test-no-106-adsorption-desorption-using-a-batch-equilibrium-method_9789264069602-en >. Acesso em: 5 de Out. de 2018.

PEREIRA-JUNIOR, E. V. et al. Effects of soil attributes and straw accumulation on the sorption of hexazinone and tebuthiuron in tropical soils cultivated with sugarcane. **Journal of Environmental Science and Health, Part B**, v. 50, n. 4, p. 238-246, 2015.

PORTAL, T. P. et al. An integrated assessment of water quality in a land reform settlement in northern Rio de Janeiro state, Brazil. **Heliyon**, v. 5, n. 3, p. e01295, 2019.

PPDB,Pesticide Properties Database. **Footprint: Creating Tools for Pesticide Risk Assessment and Management in Europe.** Developed by the Agriculture & Environment Research Unit (AERU), University of Hertfordshire, Funded by UK National Sources and the

EU-funded FOOTPRINT Project (FP6-SSP-022704). Disponível em: <http://sitem.herts.ac.uk/aeru/ppdb/en/index.htm> Acessado em: 20 de Out de 2019.

QIU, Y. et al. Competitive biodegradation of dichlobenil and atrazine coexisting in soil amended with a char and citrate. **Environmental Pollution**, v. 157, n. 11, p. 2964-2969, 2009.

RAN, Y. et al. Importance of adsorption (hole-filling) mechanism for hydrophobic organic contaminants on an aquifer kerogen isolate. **Environmental Science & Technology**, v. 38, n. 16, p. 4340-4348, 2004.

REHAN, M. et al. Opening the s-triazine ring and biuret hydrolysis during conversion of atrazine by Frankia sp. strain EuI1c. **International Biodeterioration & Biodegradation**, v. 117, p. 14-21, 2017.

REID, B. J. et al. Influence of biochar on isoproturon partitioning and bioaccessibility in soil. **Environmental Pollution**, v. 181, p. 44-50, 2013.

RHODES, R. C. Soil studies with carbon-14-labeled hexazinone. **Journal of Agricultural and Food Chemistry**, v. 28, n. 2, p. 311-315, 1980.

SHANER, D. L. et al. **Herbicide handbook**. Weed Science Society of America, 2014.

SILVA, T. S. et al. Use of neural networks to estimate the sorption and desorption coefficients of herbicides: A case study of diuron, hexazinone, and sulfometuron-methyl in Brazil. **Chemosphere**, v. 236, p. 124333, 2019.

SULIMAN, W. et al. Influence of feedstock source and pyrolysis temperature on biochar bulk and surface properties. **Biomass and Bioenergy**, v. 84, p. 37-48, 2016.

TAHIR, M. et al. Sorption and leaching potential of isoproturon and atrazine in low organic carbon soil of Pakistan under a wheat-maize rotation. **Pedosphere**, v. 26, n. 5, p. 687-698, 2016.

TRIGO, C. et al. Influence of pyrolysis temperature and hardwood species on resulting biochar properties and their effect on azimsulfuron sorption as compared to other sorbents. **Science of the Total Environment**, v. 566, p. 1454-1464, 2016.

WANG, H. et al. Modification to degradation of hexazinone in forest soils amended with sewage sludge. **Journal of Hazardous Materials**, v. 199, p. 96-104, 2012.

WANG, S. et al. Dual-template imprinted polymers for class-selective solid-phase extraction of seventeen triazine herbicides and metabolites in agro-products. **Journal of Hazardous Materials**, v. 367, p. 686-693, 2019.

WANG, X. et al. Degradation and metabolism of hexazinone by two isolated bacterial strains from soil. **Chemosphere**, v. 61, n. 10, p. 1468-1474, 2005.

WRB,I.W.G.; ISRIC, F. World reference base for soil resources. World soil resources reports,

N° 103, FAO, Rome, 2006.

WEBER, K.; QUICKER, P. Properties of biochar. **Fuel**, v. 217, p. 240-261, 2018.

XIAO, F.; PIGNATELLO, J. J. Interactions of triazine herbicides with biochar: Steric and electronic effects. **Water Research**, v. 80, p. 179-188, 2015a.

XIAO, F.; PIGNATELLO, J. J. π+–π Interactions between (hetero) aromatic amine cations and the graphitic surfaces of pyrogenic carbonaceous materials. **Environmental Science & Technology**, v. 49, n. 2, p. 906-914, 2015b.

YAVARI, S. et al. Degradation of imazapic and imazapyr herbicides in the presence of optimized oil palm empty fruit bunch and rice husk biochars in soil. **Journal of Hazardous Materials**, v. 366, p. 636-642, 2019.

YUAN, H. et al. Influence of pyrolysis temperature on physical and chemical properties of biochar made from sewage sludge. **Journal of Analytical and Applied Pyrolysis**, v. 112, p. 284-289, 2015.

ZHANG, P. et al. Adsorption and catalytic hydrolysis of carbaryl and atrazine on pig manure-derived biochars: impact of structural properties of biochars. **Journal of Hazardous Materials**, v. 244, p. 217-224, 2013.

ZHAO, B. et al. Effect of pyrolysis temperature, heating rate, and residence time on rapeseed stem derived biochar. **Journal of Cleaner Production**, v. 174, p. 977-987, 2018.

ZHELEZOVA, A. et al. Effect of biochar amendment and ageing on adsorption and degradation of two herbicides. **Water, Air, & Soil Pollution**, v. 228, n. 6, p. 216, 2017.

FINAL CONSIDERATIONS

The present study demonstrated that pyrolysis temperature has an important influence on eucalyptus wood-derived biochar properties. Temperature was positively correlated with pH, conductivity, ash content and elemental carbon; and negatively correlated with yield, volatile materials, oxygen, elemental hydrogen and H/C, O/C and (O + N) /C ratio and specific surface area.

With increasing temperature there was a reduction of surface chemical groups, loss of surface layers and formation of a stable carbon. At temperatures of 450 and 550 °C, the biochars produced have an aliphatic, polar structure and acidic pH due to incomplete biomass degradation. While biochars produced at higher temperatures (650, 750, 850 and 950 °C) have a more aromatic, more apolar structure and a more basic pH.

The properties of biochar derived from eucalyptus wood revealed that this material could be considered promising for the immobilization of various contaminants, which was confirmed in our study for the herbicide hexazinone. Increased biochar production temperature increased hexazinone sorption. Biochar produced at pyrolysis temperature of 950 °C achieved the highest sorption and lowest desorption of hexazinone, due to a higher ratio of (N + O)/C and ash content, and a lower H/C ratio. This research has shown that the H/C ratio was one of the main factors that promoted lower sorption and higher desorption of hexazinone in biochar produced at 650 °C.

Biochar produced at higher temperature contributed to minimize hexazinone leaching and distribution in soil. Higher sorption, although beneficial as it contributes to environmental decontamination, can reduce herbicide availability and diminish its efficiency in weed control.

APPENDIX

Appendix. Pearson correlation analysis of the physicochemical properties of eucalyptus-derived biochars produced at different pyrolysis temperatures.

	EC	pH	C	H	N	O	H/C	O/C	N/C	(O+N)/C	Lignin	Cellulose	870	MV	SSA	VM	Ash
EC	1.00	-0.72	-0.52	-0.92	0.64	0.38	-0.92	0.35	0.92	0.97	0.38	-0.19	-0.56	-0.76	-0.98	-0.60	0.93
pH	-0.72	1.00	0.64	0.49	-0.19	-0.57	0.50	-0.43	-0.50	-0.82	-0.71	0.59	0.03	0.77	0.84	0.19	-0.51
C	-0.52	0.64	1.00	0.15	0.32	-0.99	0.16	-0.97	-0.16	-0.68	-0.96	0.91	-0.40	0.95	0.51	-0.37	-0.18
H	-0.92	0.49	0.15	1.00	-0.89	0.01	1.00	0.00	-1.00	-0.81	0.01	-0.21	0.84	0.46	0.87	0.85	-1.00
N	0.64	-0.19	0.32	-0.89	1.00	-0.46	-0.89	-0.46	0.89	0.46	-0.45	0.61	-0.99	0.00	-0.61	-0.99	0.88
O	0.38	-0.57	-0.99	0.01	-0.46	1.00	0.00	0.98	0.00	0.56	0.97	-0.95	0.54	-0.88	-0.38	0.52	0.02
H/C	-0.92	0.50	0.16	1.00	-0.89	0.00	1.00	0.00	-1.00	-0.82	0.00	-0.20	0.83	0.46	0.88	0.85	-1.00
O/C	0.35	-0.43	-0.97	0.00	-0.46	0.98	0.00	1.00	0.00	0.52	0.90	-0.89	0.50	-0.86	-0.31	0.52	0.01
N/C	0.92	-0.50	-0.16	-1.00	0.89	0.00	-1.00	0.00	1.00	0.82	0.00	0.20	-0.83	-0.46	-0.88	-0.85	1.00
(O+N)/C	0.97	-0.82	-0.68	-0.81	0.46	0.56	-0.82	0.52	0.82	1.00	0.58	-0.40	-0.36	-0.88	-0.97	-0.42	0.83
Lignin	0.38	-0.71	-0.96	0.01	-0.45	0.97	0.00	0.90	0.00	0.58	1.00	-0.98	0.55	-0.87	-0.44	0.48	0.02
Cellulose	-0.19	0.59	0.91	-0.21	0.61	-0.95	-0.20	-0.89	0.20	-0.40	-0.98	1.00	-0.71	0.76	0.25	-0.64	0.18
870	-0.56	0.03	-0.40	0.84	-0.99	0.54	0.83	0.50	-0.83	-0.36	0.55	-0.71	1.00	-0.10	0.49	0.97	-0.82
TPV	-0.76	0.77	0.95	0.46	0.00	-0.88	0.46	-0.86	-0.46	-0.88	-0.87	0.76	-0.10	1.00	0.76	-0.06	-0.48
SSE	-0.98	0.84	0.51	0.87	-0.61	-0.38	0.88	-0.31	-0.88	-0.97	-0.44	0.25	0.49	0.76	1.00	0.58	-0.89
VM	-0.60	0.19	-0.37	0.85	-0.99	0.52	0.85	0.52	-0.85	-0.42	0.48	-0.64	0.97	-0.06	0.58	1.00	-0.84
Ash	0.93	-0.51	-0.18	-1.00	0.88	0.02	-1.00	0.01	1.00	0.83	0.02	0.18	-0.82	-0.48	-0.89	-0.84	1.00

Values in red is significant ($p \leq 0.05$).